Yale University

EliScholar – A Digital Platform for Scholarly Publishing at Yale

Yale Medicine Thesis Digital Library

School of Medicine

January 2023

Utility Of Shear Wave Elastography In Breast Cancer Diagnosis: A Systematic Review And Meta-Analysis

Aishwarya Pillai

Follow this and additional works at: https://elischolar.library.yale.edu/ymtdl

Recommended Citation

Pillai, Aishwarya, "Utility Of Shear Wave Elastography In Breast Cancer Diagnosis: A Systematic Review And Meta-Analysis" (2023). *Yale Medicine Thesis Digital Library*. 4193.
https://elischolar.library.yale.edu/ymtdl/4193

This Open Access Thesis is brought to you for free and open access by the School of Medicine at EliScholar – A Digital Platform for Scholarly Publishing at Yale. It has been accepted for inclusion in Yale Medicine Thesis Digital Library by an authorized administrator of EliScholar – A Digital Platform for Scholarly Publishing at Yale. For more information, please contact elischolar@yale.edu.

Utility of Shear Wave Elastography in Breast Cancer Diagnosis:

A Systematic Review and Meta-Analysis

A Thesis Submitted to the Yale University School of Medicine in Partial Fulfillment of the Requirements for the Degree of Doctor of Medicine

by

Aishwarya K. Pillai, 2023

Supervised by

Dr. Jonathan Langdon

UTILITY OF SHEAR WAVE ELASTOGRAPHY IN BREAST CANCER DIAGNOSIS: A SYSTEMATIC REVIEW AND META-ANALYSIS

Aishwarya Pillai[1], Teja Voruganti[1], Richard Barr[2], and Jonathan Langdon[1].

[1]Department of Radiology, Yale University School of Medicine, New Haven, CT. [2]Department of Radiology, Northeastern Ohio Medical University, Rootstown, OH

In the United States, breast cancer is one of the most diagnosed cancers in women. Early detection, often via mammography, and intervention have been shown to reduce mortality. However, not all cancers are mammographically evident in early stages, if at all. As a result, ultrasound has been increasingly used to supplement mammography for breast cancer detection and assessment, particularly in dense breasts. Recent advancements in ultrasonography include the ability to characterize the stiffness of biological tissues. Shear Wave Elastography (SWE) is one such development used to quantify tissue stiffness within a region of interest.

The resistance of soft tissue to deformation depends on the molecular makeup of the tissue components as well as elements of tissue structure, such as stromal and connective tissue. As tumor growth often involves architectural changes that cause increased stiffness compared to normal neighboring tissue, SWE has the potential to compliment mammography and B-mode ultrasound for breast lesion characterization. Studies establishing the clinical value of SWE may aid in its incorporation into diagnostic guidelines.

This study aimed to quantify the performance of 2D SWE for differentiating benign and malignant breast lesions in women with abnormal mammography via a systematic review of the literature and meta-analysis. A systematic search of PubMed,

Scopus, Embase, Ovid-Medline, Cochrane Library and Web of Science was performed. Studies of diagnostic accuracy published prior to June 2021 using SWE to evaluate abnormal breast tissue with at least 50 lesions that reported quantitative shear wave speed (SWS) parameters (the mean (SWS_{mean}), maximum (SWS_{max}), minimum (SWS_{min}), or standard deviation (SWS_{SD}) of the SWS) and thresholds and included a reference standard of either biopsy or 2-year stability were included in the analysis. The QUADAS-2 tool was used to assess possible bias within studies as well as their applicability.

87 studies of diagnostic accuracy were included, encompassing 17,810 women (47) with 19,043 lesions (7,623 malignant). A hierarchical summary receiver operating characteristic model produced the following summary sensitivities and specificities: 0.86 [0.83, 0.88] / 0.87 [0.84, 0.88] for SWS_{mean}, 0.83 [0.80, 0.85]/ 0.88 [0.86, 0.90] for SWS_{max}, 0.86 [0.74, 0.93]/ 0.81 [0.69, 0.89] for SWS_{min}, and 0.82 [0.77, 0.86] / 0.88 [0.85, 0.91] for SWS_{SD}, respectively. By calculating and utilizing the resulting likelihood ratios, SWE was shown capable of downgrading BI-RADS 4a and upgrading BI-RADS 3 lesions. Thus, SWE has the potential to provide increased discriminative power in the diagnosis of breast cancer if used synergistically with mammography and B-mode ultrasound.

Current society guidelines do not provide definitive recommendations about the role of SWE in screening and diagnosis, nor its counterpart strain elastography (SE). The literature suggests that a combination of SE and SWE may provide better discriminatory power than SWE alone and serve as an adjunct to current diagnostic techniques, opening an avenue for future study.

Acknowledgement

I would like to thank Dr. Jonathan Langdon for his inspiration, support, and mentorship throughout this process. I really appreciate you being a sounding board and letting me take the lead on this project while guiding me in the right direction if I started to veer off-track. You are a veritable genius, and I am so grateful that you were willing to take the time to dive deep into the physics and mechanics of ultrasound, shear waves, and statistic analysis with me. You answered every one of my questions, as off-topic and beyond the scope of this project as they might have been. I have learned so much from your example of how to be an extraordinary research mentor, providing structure while also empowering every single member of your team to be heard and feel supported, even through the challenges of Covid-19. I am so honored to have been able to work with you and learn from you.

To Dr. Teja Voruganti, thank you for time and commitment throughout this systematic review. You did not balk at the daunting task of evaluating all of the papers, and your willingness to endure many (many) meetings and remain tenacious was a wonderful source of motivation for me, and your experience performing prior systematic reviews was also invaluable.

I would also like to thank Dr. Richard Barr for being a trailblazer in the field of breast elastography and serving as a sounding board throughout the research process.

To Judy Spak and Courtney Brombosz, thank you for organizing and leading the Evidence-Based Clinical Information Skills elective course via Zoom during the Covid-19 pandemic. Had I not taken this course, I would likely not have felt equipped to reach out to Dr. Langdon to pursue this project. Your instruction on how to strategically search and appraise literature and synthesize evidence was crucial to this project.

Thank you to the Jane Danowski Weiss Family Foundation One Year Medical Student Research Fellowship, as well as the Yale School of Medicine Office of Student Research for several Medical Student Research Training Grants which allowed me to focus my time and efforts onto my project.

Thank you to Elsevier for allowing me to reproduce figures and tables originally published in the Journal of the American College of Radiology in my thesis, as per the author rights under their publishing agreement. Tables 3-10 and Figures 3-8 within this

thesis were first published in the article “Diagnostic Accuracy of Shear-Wave Elastography for Breast Lesion Characterization in Women: A Systematic Review and Meta-Analysis” [1].

Thank you to Sir Richardson the IVth for endless cuddles, as well as judgement during moments of procrastination.

Finally, thank you to my mother, Padmini, for your unending support, love, food, and tea. You have always been up for exploring my many (many) interests with me, as arbitrary as they might be, and you have always challenged me to find my own answers which truly defines me both as a researcher and a person.

Table of Contents

Introduction

The Radiological Society of North America first detailed the need for focused breast imaging in 1924, highlighting the challenge of diagnosing early stages of breast cancer solely via palpation or inspection [2]. In 1960, Dr. Robert Egan, the "father of mammography," published a textbook describing optimal techniques and positioning in breast radiology in an attempt to dispel the taboo around the subject and enable a more widespread adoption of the practice [3].

The Health Insurance Plan of Greater New York completed a randomized clinical trial in 1973 and noted a statistically significant decrease in mortality due to breast cancer in women offered screening compared to women who were not. As a result, clinicians requested that the American College of Radiology (ACR) standardize the execution and interpretation of mammography [2].

BI-RADS Scoring and Management

In 1985, the ACR established the Breast Imaging Reporting and Data System (BI-RADS) which uses a scale from 0 to 6 to indicate suspicious findings and provide recommendations for subsequent management [2]. The ACR recommends annual mammographic screening starting at age 40 in asymptomatic women [4]. Women with abnormal results or symptomatic women, such as those with breast lumps, nipple discharge, or breast pain, undergo more detailed diagnostic mammography for further investigation.

BI-RADS 1 and 2 lesions are benign, so only routine follow-up is indicated. BI-RADS 3 lesions have a risk of malignancy less than 2%, so shortened interval follow-up

at 6, 12, and 24 months to evaluate lesion stability is recommended, though biopsy may also be considered [2]. A BI-RADS 4 score indicates a suspicious abnormality and is further delineated as A (2-10% chance of malignancy), B (10-50% chance of malignancy), or C (50-95% chance of malignancy). Further workup via biopsy is often required. A score of 5 indicates a chance of malignancy greater than 95% and is always followed by biopsy. BI-RADS 6 lesions are malignant on biopsy and require surgical excision [5].

Though mammography has a long-proven mortality benefit, it is quite subjective and, therefore, poorly specific [2]. As a result, biopsy is frequently performed with a benign result in patients with BI-RADS 4, and sometimes 3, lesions [6-8]. To minimize the frequency of biopsy and resource utilization, more objective evaluation techniques are required.

Ultrasonography

In 1965, only an estimated five hundred practitioners were using ultrasonography (US), a portable, real-time, cost-effective imaging technique, to assist with diagnosis [9]. Today, it is a ubiquitous clinical tool used to visualize structures, differentiate between soft tissue and fluid or bone, place lines and catheters, and visualize the movement of cardiac structures and blood flow in real time by cataloging shifts in frequency. It can also be used therapeutically to induce tumor destruction [10].

Discovered by Pierre and Jacques Curie in 1880, piezoelectric materials were critical to the development of US because they respond to electric fields via bulk deformation and generate electric potentials when compressed [11]. The expansion

generated by changing the voltage applied to a piezoelectric transducer causes mechanical waves that are transmitted to the body. Likewise, when the transducer is stimulated by returning pulses, the resulting voltage changes are detected, amplified, and processed to build an image based on the intensity of the returning waves.

US utilizes acoustic waves with frequencies between 1 and 20 megahertz (MHz) that travel longitudinally, along the direction of particle movement, and are either scattered, attenuated, or reflected [10]. Waves that travel through a homogenous medium attenuate as the mechanical energy of the sound wave is converted into heat or absorbed by tissue, causing a decrease in amplitude and wavelength [11].

Acoustic impedance (AI) is the resistance to the passage of US energy described by the equation:

$$z = \rho v$$

where z is the AI, ρ is tissue density, and v is the speed of sound in a substance. As shown in Figure 1, an "echo" is produced when the incident wave encounters a change in AI between adjacent tissues, termed an "interface," and is subsequently reflected back to the transducer. The larger the difference in AI, the greater the energy disruption with less energy transmitted and more reflected.

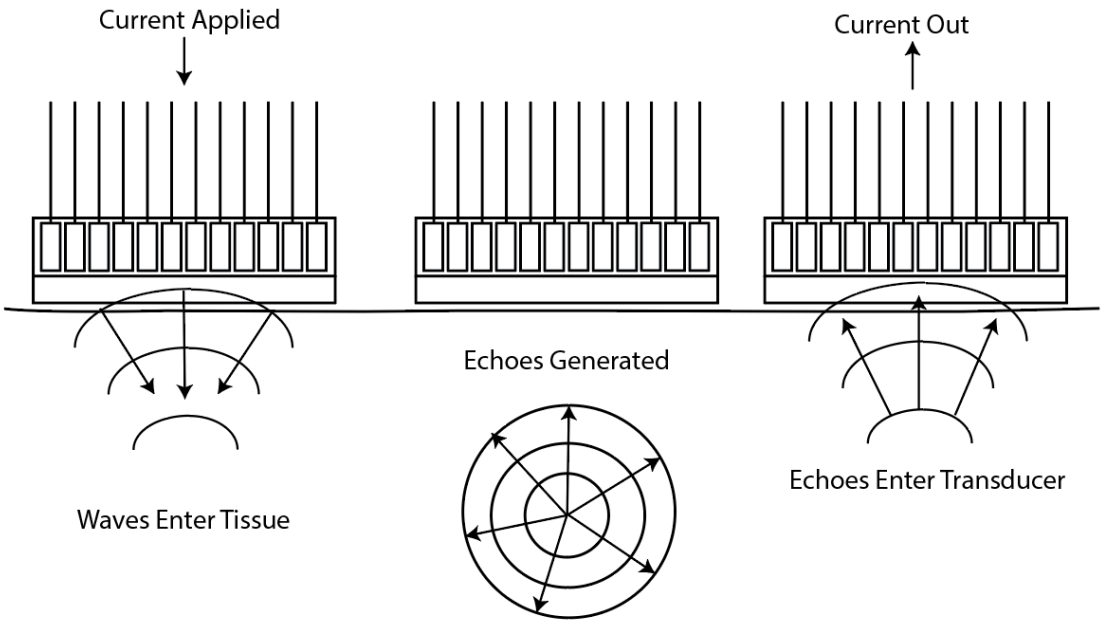

Figure 1: The piezoelectric crystals of the US transducer deform in response to the applied electric current. This generates a mechanical wave that is transferred into the skin after passing through a matching layer. Acoustic coupling with the skin surface is achieved using ultrasound coupling gel. Echoes are generated by the scattering of acoustic waves in tissue after encountering an interface. The returning waves transiently deform the transducer elements generating small voltage changes detected by the ultrasound machine.

The wave's propagation velocity or "wave speed" (WS) is determined by the density and elasticity of the tissues it travels through. For example, increased density increases the resistance of the medium to compression, thereby increasing the WS. In the body, WS can range from as low as 1410 meters/second (m/s) in fat to 1630 m/s in muscle. A value of 1540 m/s, obtained by averaging measurements from various biological tissues, is commonly used in calculations while acknowledging that measurement errors or artifacts may arise due to variations in WS [12]. The average WS and AI values of different biological tissue are shown in Table 1 [13, 14].

Table 1: Wave Speed and Acoustic Impedance Values in Commonly Imaged Biological Tissue

Tissue Type	Acoustic Impedance × 10^6 ($kg/(m^2s)$)	Wave Speed (m/s)
Air	0.0004	330
Fat	1.34	1,450
Water	1.48	1,480
Kidney	1.63	1,560
Blood	1.65	1,570
Muscle	1.71	1,580
Bone	7.8	4,080

Assuming the wave travels linearly, the presumed distance to the reflective structure can be calculated by measuring the time taken for the emitted pulse to return with the relationship

$$d = \frac{1}{2}rt$$

where d is the distance traveled, r is the WS, and t is the round-trip time from the transducer to the reflector and back. The WS of a longitudinal wave can also be related to the bulk modulus (B), a numerical constant describing the change in volume in a compressible fluid or solid under pressure on all surfaces, via the equation

$$r = \sqrt{\frac{B}{\rho}}$$

In conventional B (brightness) mode US, henceforth "US" unless otherwise specified, aggregating multiple echoes produces a two-dimensional (2D) morphological construct of the area of interest plotted via grayscale on a display [15]. Black indicates no returning echoes, such as due to air or fluid, while white represents highly echogenic interfaces [10].

Breast Ultrasonography

Utilizing both US and mammography when evaluating breast masses improves diagnostic accuracy and decreases the number of benign biopsies. Breast US is also advantageous for whole breast screening in patients with dense breasts, which are associated with an increased risk of breast cancer and decreased likelihood of cancer detection on mammography. For example, in a study of average-risk women with dense breast tissue, supplemental screening US found an additional 0.7 to 9.4 cancers per 1000 women [16].

As there is significant overlap in the appearance of benign and malignant lesions on imaging, management is based on the most concerning feature. Benign lesions most commonly present as oval-shaped with well-defined margins on imaging. They are often low density or fat-containing, appearing dark on US. Features that raise suspicion for malignancy include an irregular or micro-lobulated shape, spiculated margins, and parenchyma that appears distorted without a history of surgery or trauma to the region [17].

Elastography

Manual palpation is a key part of the physical exam and is often responsible for the detection of changes in tissue stiffness or elasticity in the body. However, the US Preventive Services Task Force (USPSTF), American Academy of Family Physicians (AAFP), and Canadian Preventive Task Force currently recommend against self-breast exams, and the AAFP and USPSTF found insufficient evidence to recommend or oppose clinical breast exams (CBE). Studies show that while CBE is very specific (94-99%), it

has a low sensitivity (21-54%) meaning that the absence of a mass on CBE does not necessarily indicate the absence of breast cancer [18, 19]. As US does not provide information about tissue elasticity, elastography aims to fill this gap, acting as a more objective method of palpation with the additional benefit of deeper penetration [20].

Elastography builds upon the foundation of US and measures tissue stiffness via strain elastography (SE) or shear wave elastography (SWE). Its utility is based on the premise that the elastic moduli of soft tissue depends on the molecular makeup of tissue components and aspects of tissue structure, such as stromal and connective tissue. Tumor growth often involves architectural changes which cause increased stiffness compared to normal neighboring tissue. A retrospective study of 348 breast lesions found that 70.2% of high-density masses were malignant (P<.0001)[1, 15].

Shear is defined as a change in shape without a change in volume due to equal forces acting in opposite directions along opposing faces of a substance. Since cells contain large quantities of water and most biological soft tissue has a bulk modulus within 15% of that of water, it is easier to alter the shape of tissue rather than the volume [12]. The shear modulus (G) describes a substance's response to shear stress. Poisson's ratio (v), usually between 0.49 and 0.499 in biological tissue, can be used to relate the shear modulus and Young's modulus (E), which describes a material's response to axial stress (from a perpendicular force), via:

$$E = 2G(1 + v)$$

Young's modulus is defined as:

$$E = \frac{stress}{strain}$$

and varies directly with compression pressure and inversely with the resulting deformation as described by:

$$stress = \frac{Force}{area} \text{ and } strain = \frac{change\ in\ length}{original\ length}$$

Both moduli have a more dynamic range than the bulk modulus, varying over several orders of magnitude. Thus, the contrast resolution of elastography is significantly greater than that of US, with the potential benefit of increased sensitivity and specificity for evaluating tissue stiffness and characterizing lesions [12]. Samani et al. measured 169 breast tissue samples with a range of benign and malignant breast tumors and varying ratios of fat and fibroglandular tissue to identify Young's modulus values in normal and diseased breast tissue. The results of this analysis are shown in Table 2 [21].

Table 2: Elastic moduli of normal and pathological human breast tissue. Adapted from Samani et al.

Breast Tissue Type	Young's modulus (kPa) [mean ± STD]
Normal Fat	3.25 ± 0.91
Normal Fibroglandular Tissue	3.24 ± 0.61
Fibroadenoma	6.41 ± 2.86
Fibrocystic Disease	17.11 ± 7.35
Low-grade Invasive Ductal Carcinoma (IDC)	10.40 ± 2.60
Intermediate-grade IDC	19.99 ± 4.2
High-grade IDC	42.52 ± 12.47
Invasive Lobular Carcinoma	15.62 ± 2.64
Ductal Carcinoma In Situ	16.38 ± 1.55

Strain Elastography

Both SE and SWE require the application of an external force, classified as quasi-static or dynamic, respectively. In SE, an external force is applied either via physiologic motion from respiratory movements or through manual transducer compression. Tissue displacement is measured by calculating the difference in position before and during compression [22]. As the strain depends on the stress applied, which is generally operator

dependent and unknown, SE cannot be used to calculate Young's modulus. Instead, a qualitative strain map, also known as an elastogram, is generated by comparing the strain in the lesion to that of normal surrounding tissues. This data is then overlaid over an US image, indicating the relative stiffness between adjacent tissues [23, 24]. This technique is used commercially by Hitachi in their "Real-time Tissue Elastography" instrument [20].

Shear Wave Elastography

SWE, unlike SE, produces quantitative results [24]. It can be further divided into transient elastography (TE) and acoustic radiation force impulse (ARFI) imaging. The technique begins with the application of a vibration (TE) or longitudinal acoustic radiation force (ARFI) at frequencies between 10 - 2000 Hz (due to absorption at higher frequencies) that causes transverse particle displacement. If the substance is elastic, it will regain its original shape after the initial disturbance. Contiguous particles will undergo the same experience, with the resulting "shear wave" travelling parallel to the tissue and perpendicular to the transducer, as shown in Figure 2.

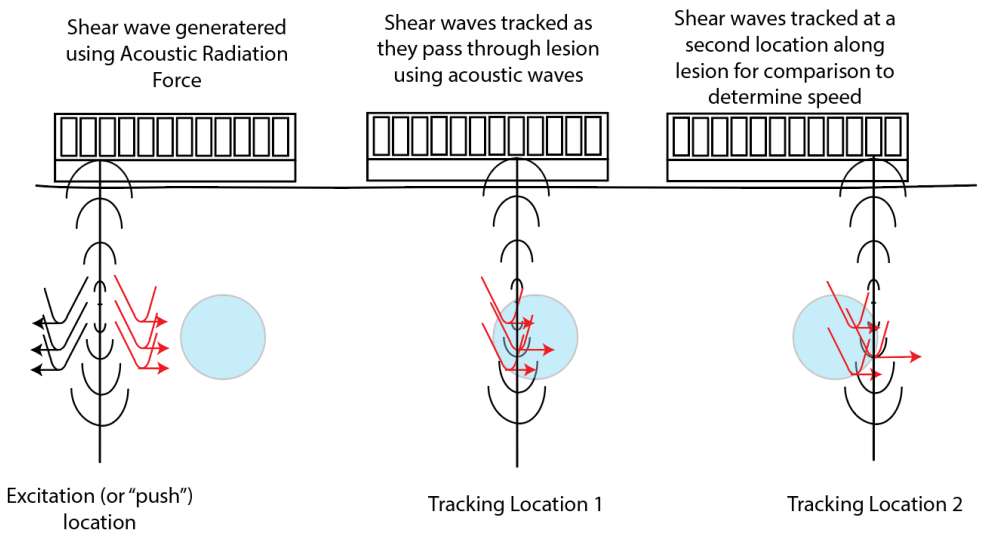

Figure 2: Applying an acoustic radiation force or push pulse causes transient transverse particle displacement which is, in turn, transmitted to contiguous tissue particles. The shear waves travel perpendicular to the transducer, speeding up when they encounter substances with greater stiffness and slowing when they encounter less stiff materials. This data is collected by a receiver and used to calculate Young's modulus. In this model, a single push location and two tracking locations are utilized. However, different manufacturers may use different quantities and combinations of push and tracking locations.

The WS of shear waves, termed shear wave speed (SWS) is described by:

$$SWS = \sqrt{\frac{G}{\rho}}$$

Under the assumption that (1) biological tissue is incompressible (Poisson's ratio of ~0.5), (2) tissue density can be approximated to that of water $\left(\rho = 1 \frac{\text{kg}}{\text{m}^3}\right)$, and (3) the force applied and resulting deformations are modest, the shear modulus, Young's modulus, and SWS (often between 1-50 m/s) can be related using

$$E = 3G = 3\rho c^2 \text{ [25, 26]}$$

Since shear waves are significantly slower than longitudinal compression waves, the transmitted waves are uncoupled from the reflected waves, allowing the same transducer to be used to generate shear waves and image their propagation [20]. The transient tissue displacement and strain are detected within the region of interest (ROI)

and used to calculate the mean, minimum, maximum, and standard deviation of the SWS (SWS_{mean}, SWS_{min}, SWS_{max}, SWS_{SD}). Often, these values are also automatically converted to the respective elasticity value (E_{mean}, E_{min}, E_{max}, E_{SD}).

In TE, shear waves are generated externally by a mechanical vibrating device mounted on an US transducer [27]. The acquisition time is often less than 100 milliseconds (ms), so measurements can be made for static and dynamic organs [28]. However, TE is limited in that it does not facilitate ROI selection, nor can the acquired data be oriented using an US image. Penetration depth is also often insufficient in patients with an increased body mass index (BMI) [29].

In contrast, ARFI imaging can be performed alongside US imaging. A short duration (0.1-0.5 ms) acoustic radiation force, termed a "push pulse," is applied to induce displacement of adjacent tissue within a specific ROI [30]. Unlike TE where shear waves are generated at the skin-air interface, ARFI produces shear waves that originate within the body, reducing, but not eradicating, the effects of elevated BMI [31].

ARFI-Based Techniques

A number of commercial systems utilizing ARFI imaging have been developed.

The Siemens Virtual Touch™ Imaging (VTI) system uses ARFI as an alternative method for generating strain, thereby addressing the operator dependence that limits conventional SE [31]. The ARFI-induced displacement and relaxation time within an ROI is measured as it is in SE and displayed as an elastogram overlaid on an US image.

Point SWE (pSWE) uses ARFI to generate quantitative results by applying a push pulse to a single location within a small ROI (often several millimeters) and measuring

the SWS. As only a single SWS measurement is generated per acquisition, this technique does not produce an image. The Virtual Touch™ Quantification (VTQ) system by Siemens and the Elast-PQTM system by Philips are two commercial applications of this technique.

Newer techniques measure the SWS in a 2D region (approximately 2-3 cm per side) using multiple successive ARFI excitations that sweep across the ROI. Following each excitation, the shear wave propagation is tracked at two different lateral tracking locations to calculate the transit time of the shear wave between those locations as a function of depth. This data is then used to calculate SWS and Young's modulus [32]. A shear wave quality map is often captured to allow the operator to modify the measurement ROI, which is extracted from the full 2D-SWE image, using both anatomical insights and tissue stiffness data to optimize imaging. The Virtual Touch™ Imaging Quantification (VTIQ) system by Siemens uses this technology, incorporating quantitative and relative stiffness information into a color-coded 2D image that indicates tissue stiffness within the ROI in m/s [31, 33].

Supersonic shear imaging (SSI) combines aspects of TE and ARFI by focusing multiple push beams at different depths. Constructive interference of the spherical waves induced by each beam increases their amplitude and speed to generate a supersonic shear source. Ultrafast plane wave imaging with a high pulse-repetition-frequency (PRF) and an approximate frame rate of 5000 images per second is required alongside beamforming, a technique used to focus signals to specific locations, to monitor shear wave propagation [30]. Data acquisition can be completed in less than 30 ms, enabling real time measurements presented on a color display of stiffness values. SSI can image a larger

ROI than earlier techniques due to constructive interference, but mainstream adoption is limited as SSI requires a special receiver capable of high PRF via synthetic aperture imaging [29]. Additionally, since SSI generates only one shear wave from multiple focused pushes which travel away from the push beam center, the SWS within the center cannot be determined due to the absence of shear waves. Therefore, multiple data acquisitions with different push locations are needed to reconstruct a complete shear map. Aixplorer's Supersonic Imagine device contains a transducer array capable of integrating the excitation and imaging functions needed for this technique.

Comb-push Ultrasound Shear Elastography (CUSE) addresses the lack of shear waves in the push beam region, facilitating the reconstruction of a larger shear map using only one acquisition. CUSE introduces push beams at different spatial locations simultaneously by transmitting an unfocused push pulse through multiple sub-apertures arranged in a comb-like formation (hence the name "comb-push"). Each beam generates two shear wave fronts that travel in opposite directions. Like in SSI, constructive interference increases their amplitude and speed. However, unlike SSI, shear waves are also generated within the beam region due to the existence of multiple simultaneous push beams, so only a single acquisition is required. A directional filter is used to remove destructive interference and extract shear waves propagating left-to-right and right-to-left [29]. Conventional US systems with low PRF can be used to quantify SWS by successively firing tracking vectors and temporally calibrating the data; information from two points at the same depth is used to calculate the local SWS of a pixel between them. [44]. These values are amalgamated to build a SWS map. Benefits of CUSE include decreased motion artifact and the ability to monitor dynamic changes in tissue properties

through rapid data acquisition and display generation (less than 35 ms). [30]. The LOGIQ E9 machine created by General Electric is the first to implement this method on a commercial US machine.

Biopsy

The standard of care for evaluating suspicious BIRADS 4 and 5 lesions is percutaneous biopsy, often performed under US guidance. Less commonly, it can be performed under MRI guidance or mammographic guidance (known as a stereotactic or tomosynthesis-guided biopsy) [34]. If suspicious findings develop in BIRADs 3 lesions during follow-up imaging at 6, 12, or 24 months, biopsy is subsequently recommended [35].

Both fine-needle aspiration (FNA) and core needle biopsy (CNB) can be performed under US guidance. During the former, a tiny needle (usually 18-25 gauge) is agitated rapidly within the lesion to collect cells. If a cytopathologist deems the cells to be sufficient, they will be further examined, and a diagnosis will be made. During the latter, a core of tissue is extracted from the target using a needle ranging in size from 9-18 gauge [2]. Several samples are collected and preserved in formalin for diagnosis. The presence or absence of malignant cells can often be determined using both methods; however, the structural details present in CNB are lost in FNA. As a result, the pathologic diagnosis in FNA is often less precise [36].

Stereotactic biopsies are generally indicated for findings not prominently apparent on US, most frequently calcifications. Two stereo X-rays are taken and used by a computer to calculate the ideal sample site. Several samples are then collected by

advancing a core needle (usually 9 gauge) to that site. An MRI-guided biopsy follows a similar procedure after administration of intravenous contrast. Both methods are effective in examining lesions that are not obvious on US but are too time-consuming for routine use [34].

Once pathology results are available, an evaluation of the radiographic-pathologic association is performed. If the pathologic findings diverge from those on imaging, a second percutaneous biopsy or surgical procedure is indicated [37].

Statement of Purpose

Multiple in vivo studies have shown that SWE can characterize breast lesions with high sensitivity and specificity since malignant lesions are often significantly stiffer than benign lesions [38-40]. However, this technique cannot be integrated into diagnostic guidelines without first establishing the significance lesion stiffness should have in deciding management. This requires (1) determining which SWS statistic (SWS_{mean}, SWS_{min}, SWS_{max}, or SWS_{SD}) is optimal to differentiate between benign and malignant breast lesions, and (2) identifying the appropriate cutoff value for the respective entity. The body of literature with regards to the use of SWE for breast lesion characterization is composed primarily of descriptions of the technique being used on phantoms, detailed breakdowns of the relevant physics concepts, and diagnostic accuracy studies which retroactively determine the most accurate cutoff value based on the data collected during the trial. However, this evidence has yet to be synthesized.

This systematic review aimed to fill this knowledge gap and allow clinicians to better incorporate SWE in the diagnostic pathway to supplement BI-RADS

categorization. We hypothesize that SWE, in conjunction with mammography, will provide the data needed to upgrade or downgrade a lesion's BI-RADS category when appropriate and reduce the need for extraneous biopsies. The specific research questions that this thesis aims to address are "what is the diagnostic performance of 2D-SWE for differentiating benign and malignant lesions, and is it possible to use existing data to determine the optimum threshold for each parameter?"

Methods

Student Contributions

This author designed the research question and objectives, identified inclusion and exclusion criteria, constructed search criteria using MESH terms, searched multiple databases, and drafted the protocol for registration into Open Science Framework. Key guidance in development of the research question and inclusion and exclusion criteria was provided by Yale Radiology Clinical Fellow Jonathan Langdon (JL), MD, PhD and Northeastern Ohio Medical University Professor of Radiology Richard Barr, MD, PhD. Registration on Open Science Framework was completed by JL. Additional technical input on optimal utilization of electronic databases to conduct the search and tools to coordinate the systematic review was provided by research librarians at the Harvey Cushing/John Hay Whitney Medical Library at the Yale University School of Medicine.

This author then performed an additional manual search, first, searching reference lists of included articles, and second, performing citation tracking. This author recruited Penn Medicine Internal Medicine resident (previously Yale School of Medicine student) Teja Voruganti (TV), MD, PhD as an additional reviewer. Both this author and TV

screened each paper that fulfilled the search criteria, first by title and abstract, then via full text for articles included on abstract according to eligibility criteria, documenting the rationale for papers that did not meet criteria. JL acted as a tiebreaker in cases of dissent. Both this author and TV also independently assessed the quality of each paper using the Quality Assessment of Studies of Diagnostic Accuracy included in Systematic Review (QUADAS-2) tool. Data extraction was performed entirely by this author and checked by JL. Statistical analysis was performed by JL. This author performed all the steps in narrative synthesis, manuscript, and thesis preparation. This author worked with JL to perform revisions and submit for publication. This work was published online in the Journal of the American College of Radiology in March of 2022, and in the May 2022 issue.

Ethics Statement

This study was not subject to Institutional Review Board (IRB) approval given that it was a systematic review of the literature with the goal of synthesizing the current state of knowledge regarding the diagnostic accuracy of SWE in the characterization of breast lesions. All data regarding human subjects was obtained from already-existing, publicly accessible data and materials that had been published in the literature and appropriately deidentified.

Human Subjects Research and Laboratory Animals

The primary method for the present study was a systematic review and meta-analysis of the literature. This work does not fall under the category of human subjects

research, so IRB approval was waived. Laboratory animals were not utilized, so approval from the Institutional Animal Care and Use Committee was not required.

Methods Description

A systematic literature search was performed, the results of which were reported according to Preferred Reporting Items for Systematic Reviews and Meta-Analyses for Diagnostic Test Accuracy (PRISMA-DTA) guidelines.

Protocol

The "Breast Elastography Meta-Analysis Study Protocol" was published in the Open Science Framework on November 28, 2020 (doi:10.17605/OSF.IO/7Z8EM). A revised protocol was uploaded in June 2021 (doi:10.17605/OSF.IO/VTD78) and can be accessed in Appendix D.

A systematic search of the medical literature was first executed in May 2020 with a final search in June 2021 to account for any applicable papers published between the initial search and the date of journal submission. To minimize the effects of publication bias and ensure a comprehensive search that appropriately captured data found in gray literature, the following databases were queried: PubMed, Scopus, Embase, Ovid-Medline, Cochrane Library and Web of Science. Additional articles were discovered by reviewing the reference lists of the articles in the initial literature search.

For article retrieval, the following search terms were employed: "elasticity imaging," "shear wave elastography," "mammary ultrasound," "breast ultrasound,"

"virtual touch tissue imaging quantification," "breast tumor," "echography," "elastography," "VTIQ," and "ultrasound."

Queries utilized the Medical Subject Headings (MeSH) thesaurus for the Medline database and the Emtree thesaurus for the Embase databases to include any article indexed with either the search term or a related term to ensure all pertinent articles were captured in the literature search. For example, searching only "elastography" does not account for other terms or phrases that also describe a class of imaging that maps tissue stiffness. The thesauri helped address this gap, as shown by the following list of linked subjects for "elastography"[MeSH Terms]":

> *Elasticity Imaging Technique; Imaging Technique, Elasticity; Imaging Techniques, Elasticity; Technique, Elasticity Imaging; Techniques, Elasticity Imaging; Tissue Elasticity Imaging; Elasticity Imaging, Tissue; Elasticity Imagings, Tissue; Imaging, Tissue Elasticity; Imagings, Tissue Elasticity; Tissue Elasticity Imagings; Elastography; Elastographies; Vibro-Acoustography; Vibro Acoustography; Vibro-Acoustographies; Magnetic Resonance Elastography; Elastographies, Magnetic Resonance; Elastography, Magnetic Resonance; Magnetic Resonance Elastographies; Resonance Elastographies, Magnetic; Resonance Elastography, Magnetic; Sonoelastography; Sonoelastographies; Acoustic Radiation Force Impulse Imaging; ARFI Imaging; ARFI Imagings; Imaging, ARFI; Imagings, ARFI; Elastograms; Elastogram*

Only articles in English or with English translations were considered. All articles were imported into EndNote 20 and the "Find Duplicates" function was used to eliminate duplicates. Two authors (AP and TV) independently assessed the remaining articles by title and abstract.

Studies were included if they constituted original research articles describing diagnostic accuracy studies that included a comparison of SWE to the current gold standard of either biopsy or 2-year stability in women with suspicious breast lesions. Though men can also develop breast cancer, most of the articles recovered in the search sampled only women. Therefore, to increase extrinsic viability, the population for this review was limited to women. Studies were eligible for inclusion if they fulfilled the following criteria:

- *Original research article*
- *Utilized a reference test for diagnosis (histologic analysis of a core-needle biopsy specimen or surgical specimen or mammographic and clinical follow-up proving 2-year stability of the lesion)*
- *Presented the results as a SWS, Shear Modulus, or Young's Modulus value or provided data allowing for their calculation*
- *Examined both malignant and benign lesions*
- *Described the statistics and thresholds used to differentiate benign and malignant lesions, including the mean, minimum, maximum, or standard deviation parameters (SWS_{mean}, SWS_{min}, SWS_{max}, or SWS_{SD}) in the described ROI*
- *Included at least 50 cases*

Review articles, case reports, letters, editorials, and studies with clinically selected populations were excluded. Though review articles were excluded, the articles summarized in these reviews were screened for possible inclusion. Due to the variation in study reporting, there were some studies that did not independently report the accuracy of SWE alone, instead examining the accuracy of SWE combined with B-mode US, for example. These studies were excluded from the meta-analysis, though it is acknowledged that were SWE to be implemented in diagnostic guidelines, these technologies would

likely be combined and aid in diagnostic accuracy. Studies utilizing pSWE techniques were also excluded.

Disagreements between the reviewers were either resolved through discussion or, if agreement remained elusive, by consulting a third team member (JL), with the majority opinion used for analysis. Full texts of relevant studies were then evaluated. Study quality, including applicability and the risk of bias, was assessed by both reviewers (AP and TV) using the QUADAS-2 tool.

Data extraction was performed solely by this author. The data collected consisted of the following, when available:

- *study design*
- *year of publication*
- *bibliographic data*
- *number of patients*
- *age range and mean age*
- *type of lesion*
- *range of lesion diameter*
- *prevalence of malignant lesions*
- *SWS, Shear Modulus, or Young's Modulus threshold values*
- *cutoff values*
- *ROI size*
- *diagnostic sensitivity and specificity of 2D-SWE*
- *brand of imaging machine used*

The initial aim of this systematic review was to evaluate studies that defined a cutoff value prior to experimentation and applied it prospectively to determine the accuracy of their hypothesized ideal threshold. However, only two studies with this aim were found in the literature, both of which used 50 m/s as the cutoff threshold for SWE_{mean}. Upon encountering this complication, the purpose of this systematic review was

amended to analyze studies that retroactively determined a cutoff value by comparing the collected SWE values and the final diagnosis, either by biopsy or 2-year stability, in order identify a cutoff value for prospective evaluation in future studies.

Since all but 12 of the studies utilized either the Aixplorer US system or the Acuson S3000 US system, a subgroup analysis of the diagnostic accuracy of SWE was performed for each device to determine whether the system and minor variations in the technique used impacted the calculated cutoff value. The few studies that did not use either system were excluded from this analysis.

Additionally, a few studies assessed multiple evaluation criteria within the same imaging modality which produced several sets of threshold values and associated sensitivities and specificities. In these instances, each data set was evaluated within the context in which it was collected to decide which set of values would be included in the final analysis.

To provide the general demographics of the patients included in this study, the composite age of all patients reported was calculated by using the reported mean ages, if this information was available. If the study reported the median rather than the mean age, the sample was assumed to be normally distributed, and the median was substituted for the mean when calculating a composite mean across all of the included studies.

Statistical Methods

Most studies incorporated in this analysis reported a sensitivity and specificity for all four SWS parameters: SWS_{min}, SWS_{mean}, SWS_{max}, and SWS_{SD}. Thresholds reported as Young's Modulus or Shear Modulus values were converted to SWS using the

relationships discussed in the introduction. These statistics were analyzed independently for each parameter to generate summary statistics and processed via a hierarchical summary receiver operating characteristic (HSROC) analysis using the statistical software suite SAS via METADAS (an SAS macro made to automate the fitting of HSROC models for meta-analysis of diagnostic accuracy studies) developed by Jonathan Deeks [41, 42]. HSROC uses two levels to model the statistical distribution of data and generate an asymmetric receiver operating characteristic (ROC) curve that allows for variation in test stringency and accuracy between studies. The first level models the 2x2 tables in each included study to evaluate within-study variability. The second level models between-study variability (heterogeneity) to account for non-independence of sensitivity and specificity across studies [41]. Pooled sensitivity and specificity values, a 95% confidence region, and a 95% prediction interval were calculated, and these results, along with those from the vendor specific subgroup analysis, are provided below.

To account for the possibility of publication bias, as studies with positive results are more likely to be submitted and published compared to studies describing negative or neutral results, funnel plot tests were performed to assess for "missing studies." In the absence of publication bias, the plot is expected to look like an inverted funnel. If publication bias is present, asymmetry will be evident. Begg's rank test was also used to assess whether there was a significant correlation between effect sizes and corresponding sample variance.

Results

Literature Search

The search strategy yielded 2,750 records (1,711 after duplicate removal). 1,529 studies which examined SE or a combination of 2D-SWE and other technology, were review studies or meta-analyses, evaluated alternate cancers, or had less than 50 participants were excluded during the initial review of title and abstract. Full-text analysis was performed on 182 articles, with 87 identified as relevant to the research topic and meeting all inclusion criteria. A PRISMA flow diagram detailing article selection is shown in Figure 3. Per the QUADAS-2 tool, the quality of studies was generally high.

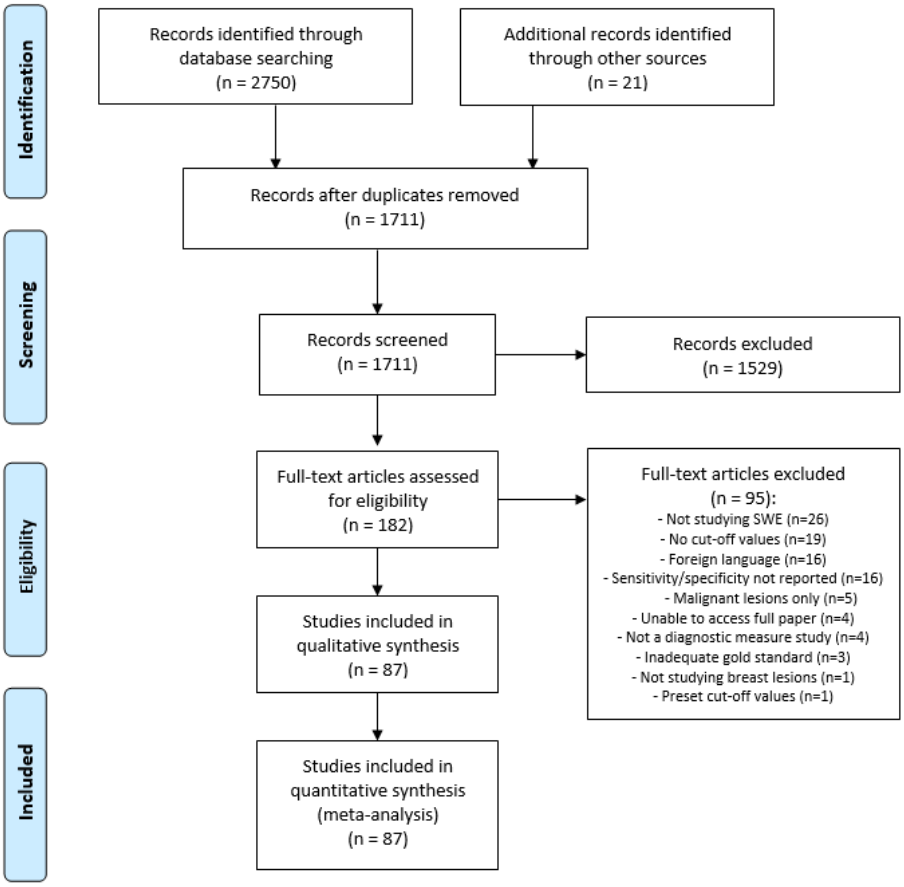

Figure 3: Article selection for meta-analysis

Data collection within these studies occurred from 2010 to 2021 (median year, 2017). All studies were diagnostic accuracy studies, and though there was inter-study design variability, most utilized the following framework:

- Patients were enrolled within several weeks to months
- Standard B-mode US was used for BI-RADs classification of lesions
- SWE was performed
- The final diagnosis was determined via biopsy or 2-year stability
- The ROC was plotted
- The diagnostic performance of the elastography parameters were calculated according to the sensitivity, specificity, positive predictive value, and negative predictive value
- SWE results were compared with the histopathologic results to derive a cut-off value

Most studies used US-guided core biopsy with or without surgical excision as a reference standard. 2-year stability via US follow-up was used to monitor lesions characterized as benign in 10 of the included studies. Though all studies used 2D SWE as the index test, they did not all use the same machine, so the acquisition method may have varied.

A complete list of the studies included in the final analysis, along with characteristics of the studies (e.g. number of patients, average age, number of lesions, reference standard, BI-RADS categories included, and ultrasound system used), and the results of their QUADAS-2 assessments are available in Appendix A, B, and C, respectively.

Demographic Data

Overall, 17,810 patients with 19,043 lesions (7,623 malignant) were analyzed. Of the patients for whom data about age was available, the composite mean age was 47 years, as shown in Table 3. Lesion sizes ranged from 1.3 mm to 111 mm.

Table 3: Combined Demographics of the Studies Included in the Meta-Analysis

Demographic Category	Quantity
Total Patients:	17,810
Total Lesions:	19,043
Malignant:	7,623
Benign:	11,420
Mean Patient Age:	47

ROI Determination

The ROIs used within studies that reported these data were inconsistent, likely because no standard method for determining the ROI currently exists in the literature. For example, some studies used circular ROIs with diameters ranging from 1-3 mm while others used square or rectangular boxes with dimensions ranging from 1 mm x 1 mm to 3 cm x 2.5 cm. Given that most studies in the meta-analysis imaged a 2 mm ROI, the values associated with this ROI were chosen for inclusion if data for multiple ROIs was provided.

Studies with Multiple Data Sets

The following studies investigated multiple evaluation criteria resulting in several sets of threshold values with associated sensitivities and specificities. The rationale for the data set chosen for inclusion in the final meta-analysis is described below.

Chen et al.[43] reported separate data sets for lesions less than 10 mm, between 10-20 mm, and greater than 20 mm. To incorporate these results into the analysis, the 2x2

tables for each grouping were combined, and this pooled data set was included in the final analysis. Hong et al. and Yang et al. both reported results for two observers, so the averages of their sensitivities, specificities, and thresholds were calculated and included in the final analysis [44, 45].

Golatta et al. reported a data set based on the Youden J statistic and another based on a threshold the author believed would optimize sensitivity [46]. As the former was more similar to the methods used by other studies in this meta-analysis, the associated data set was chosen for analysis. Ianculescu et al. reported results for BI-RADS 2-5 lesions, as well as BI-RADS 4 lesions alone; the more inclusive study was chosen to better evaluate the full range of SWE's diagnostic capabilities [47]. Finally, in the case of Ren et al. which published data for both the Aixplorer and Toshiba Aplio500 devices, data for the Aixplorer device was analyzed since no other included studies reported using the Toshiba device [48].

SWE Parameters

The diagnostic odds ratio (DOR), sensitivity, specificity, positive likelihood ratio (LR+), negative likelihood ratio (LR-), and HSROC curves were generated for each SWE parameter as seen in Table 4 and Figure 4. The pooled SWS_{mean} had a DOR of 38, sensitivity of 0.86, specificity of 0.87, LR+ of 6.37, and LR- of 0.17. The pooled SWS_{max} had a DOR of 36, sensitivity of 0.83, specificity of 0.88, LR+ 6.96, and LR- 0.19. The pooled SWS_{min} had a DOR of 26, sensitivity of 0.86, specificity of 0.81, LR+ of 4.47, and LR- of 0.17. The pooled SWS_{SD} had a DOR of 34, sensitivity of 0.82, specificity of 0.88, LR+ of 7.02, and LR- 0.21.

Table 4: Meta-analysis Results (mean [95 % CI])

	# Studies	DOR	AUC	Sensitivity	Specificity	LR+	LR-
Mean	67	38.40 [28.98, 50.89]	0.93 [0.91, 0.94]	0.86 [0.83, 0.88]	0.87 [0.84, 0.88]	6.37 [5.48, 7.41]	0.17 [0.14, 0.20]
Max	61	35.74 [26.59, 48.06]	0.92 [0.90, 0.94]	0.83 [0.80, 0.85]	0.88 [0.86, 0.90]	6.96 [5.70, 8.51]	0.19 [0.17, 0.23]
Min	14	25.63 [9.33, 70.42]	0.90 [0.82, 0.96]	0.86 [0.74, 0.93]	0.81 [0.69, 0.89]	4.47 [2.65, 7.55]	0.17 [0.09, 0.34]
SD	17	33.89 [20.79, 55.25]	0.92 [0.88, 0.94]	0.82 [0.77, 0.86]	0.88 [0.85, 0.91]	7.02 [5.19, 9.49]	0.21 [0.16, 0.27]

Summary DOR, AUC, sensitivity, specificity, LR+, and LR- values were generated for each SWE parameter by pooling the data from the studies included in the meta-analysis. AUC=area under the curve.

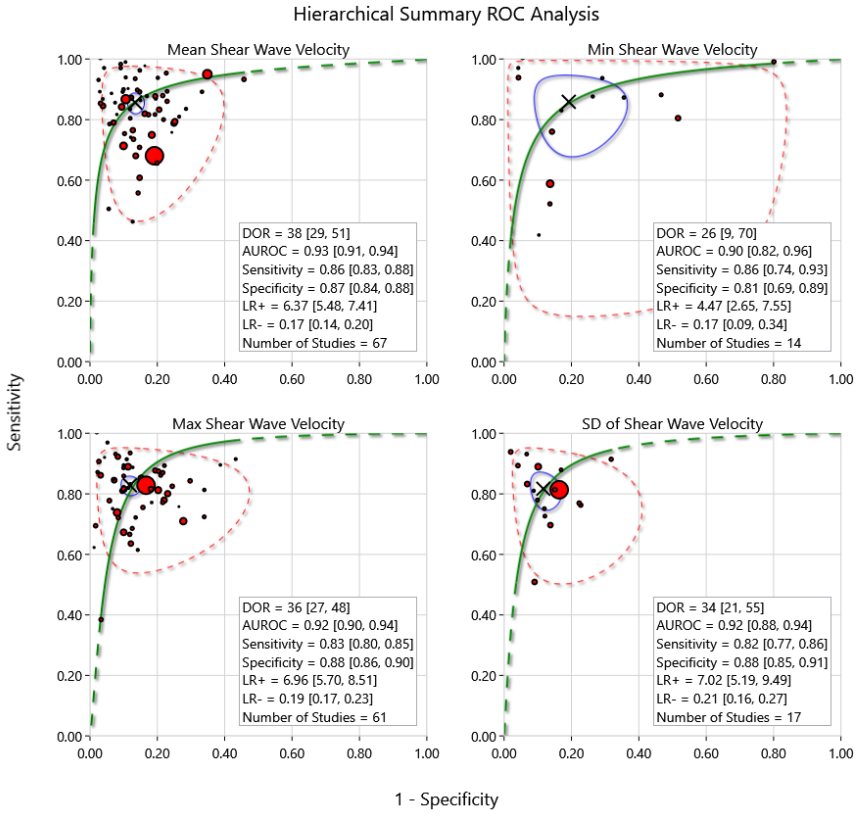

Figure 4. Results of the overall meta-analysis. Independent analyses were performed for SWS_{mean} (upper left), SWS_{min} (upper right), SWS_{max} (lower left), and SWS_{SD} (lower right) incorporating all the studies that evaluated the respective parameter. Filled red circles represent studies, with the area of each indicating the relative study size. Solid green lines provide the mean ROC fit, blue circles reflect the 95% CI, dashed red lines reflect the 95% prediction interval, and the "X" indicates the pooled sensitivity and specificity. The pooled DOR and associated AUROC, sensitivity, specificity, LR+, and LR- are shown with the 95% CI in brackets. AUROC=area under the ROC curve.

The cutoff values reported in the included studies varied widely. The thresholds used for each SWS parameter were compared with their respective DOR, sensitivity, and specificity, the results of which are displayed in Figures 5-7, respectively. Though HSROC analysis cannot be used to identify a definitive optimal cutoff value, the weighted averages and standard error thresholds for SWS_{mean}, SWS_{max}, SWS_{min}, and SWS_{SD} were 3.89 ± 1.03 m/s, 4.96 ± 0.87 m/s, 2.58 ± 0.82 m/s, and 1.79 ± 0.38 m/s, respectively.

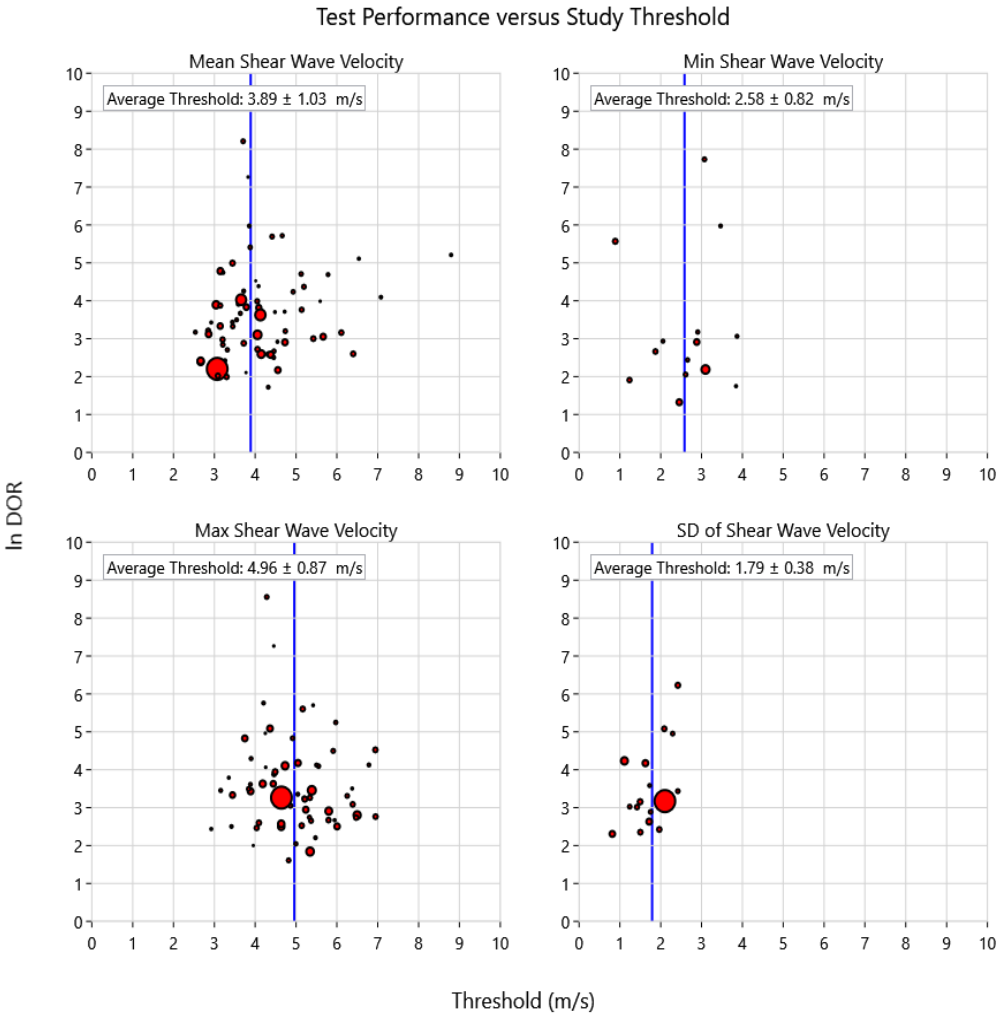

Figure 5. The relationship between cut-off values for each SWS parameter identified through the meta-analysis and the discriminative power of 2D-SWE as the natural log of the DOR. Filled red circles represent studies, with the area of each indicating relative study size. The study size-weighted average threshold for each parameter is denoted by the blue line.

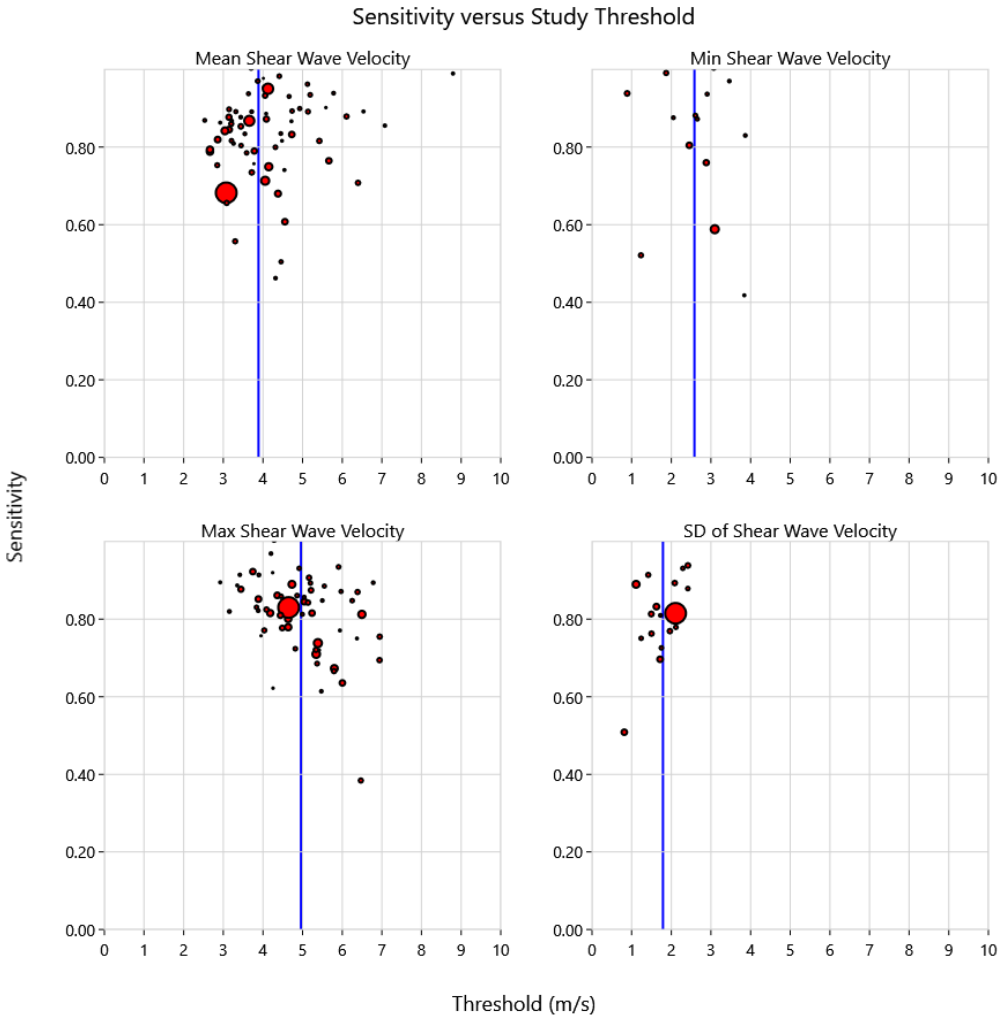

Figure 6. The relationship between cut-off values for each SWS parameter identified through the meta-analysis and the reported study sensitivity. Filled red circles represent studies, with the area of each indicating relative study size. The study size-weighted average threshold for each parameter is denoted by the blue line.

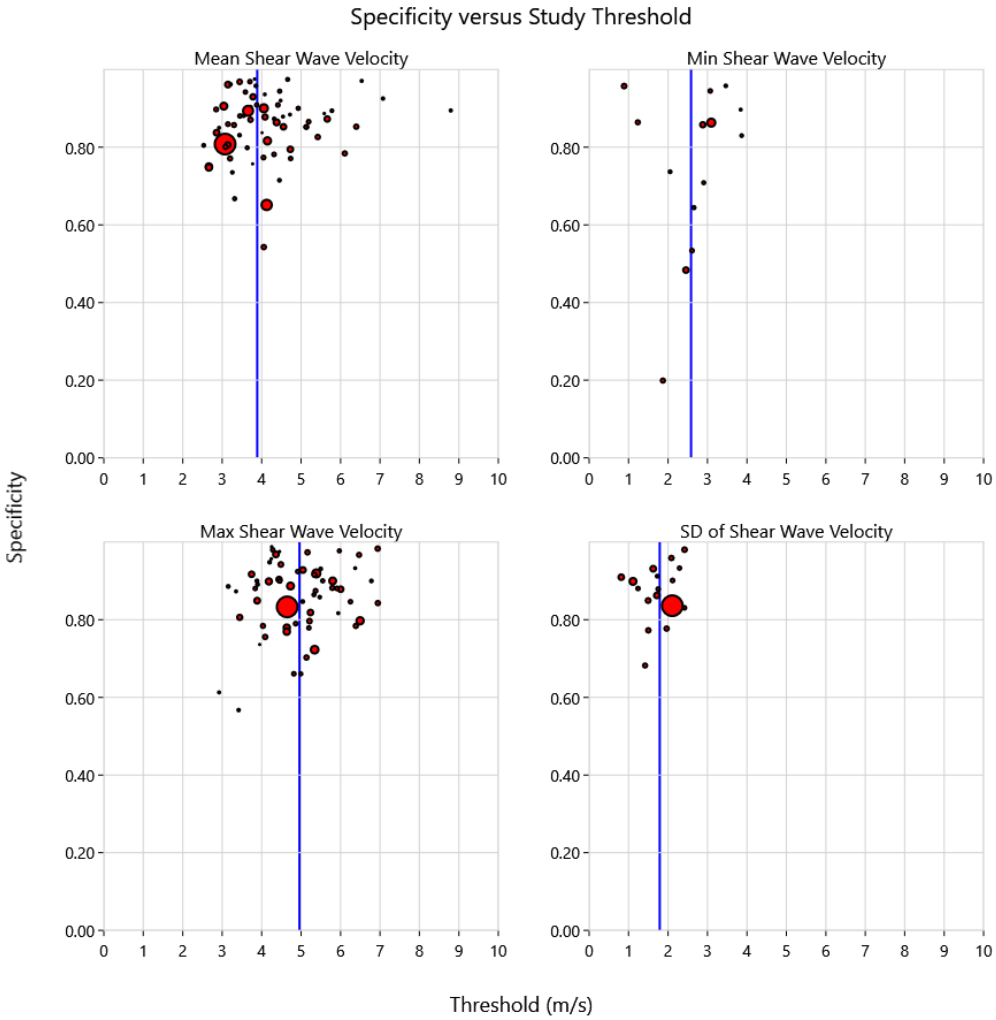

Figure 7. The relationship between cut off values for each SWS parameter identified through the meta-analysis and the reported study specificity. Filled red circles represent studies, with the area of each indicating relative study size. The study size-weighted average threshold for each parameter is denoted by the blue line.

The funnel plot analyses shown in Figure 8 demonstrate significant asymmetry, indicating the possibility of publication bias. These findings are supported by a p value < 0.05 in all subset plots by Begg's rank test for funnel plot asymmetry.

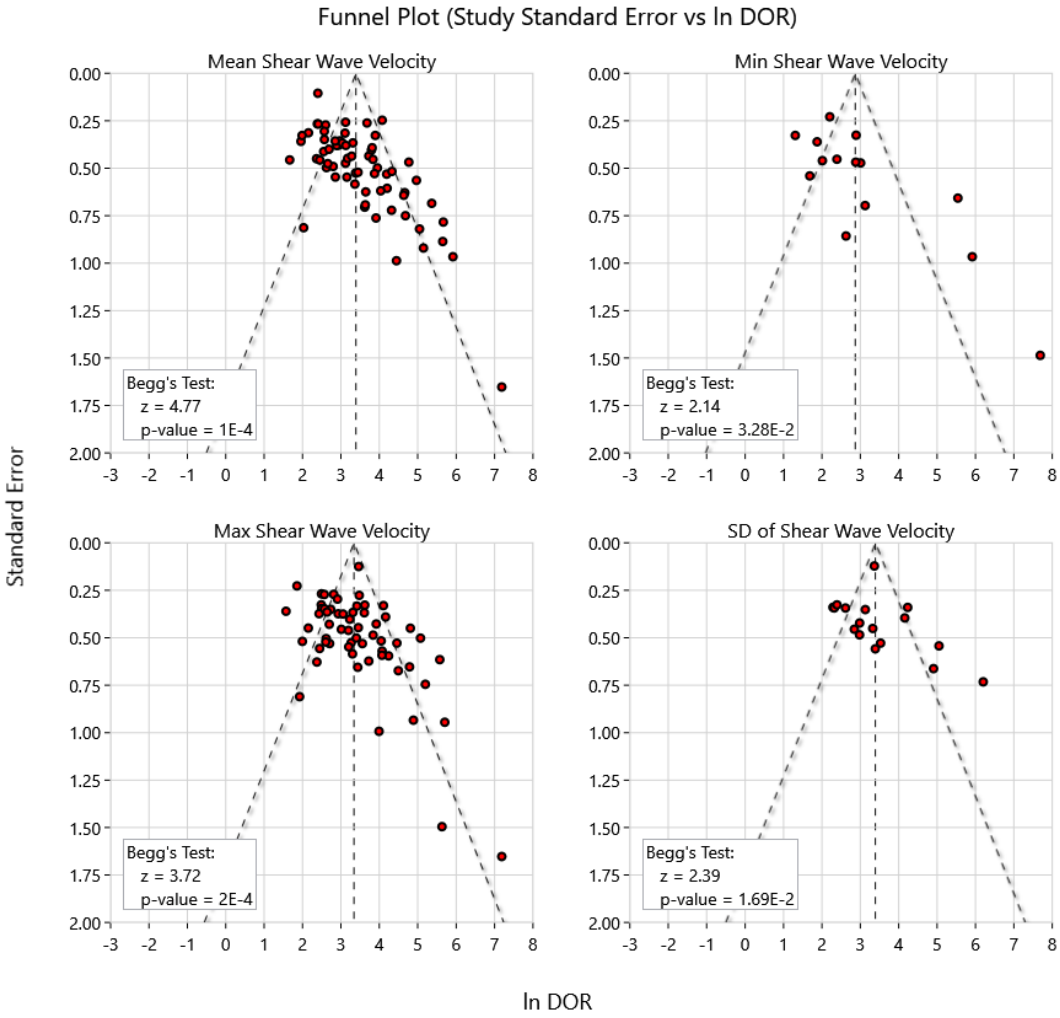

Figure 8. Funnel plots for each SWS parameter to assess for bias in the underlying data sources. Red circles represent included studies. The results of Begg's test for funnel plot asymmetry are displayed in the bottom left corner of each plot. All four plots demonstrate asymmetry with smaller studies (those with high standard error) demonstrating higher log DOR values.

Subgroup Analyses

The results of the subgroup analysis comparing the the Acuson system (28/87 studies; 32%) to the Aixplorer system (44/87 studies; 51%) displayed in Table 5 show no statistically significant differences between the two brands, though it is important to note that the analyses of SWS_{min} and SWS_{SD} are limited by low power.

Table 5: Sub-group Analysis – Aixplorer SuperSonic Imagine versus Siemens Acuson

	Brand	#	DOR	AUC	Sensitivity	Specificity	LR+	LR-
Mean	Aixplorer	33	35.16 [23.60, 52.39]	0.91 [0.88, 0.94]	0.87 [0.82, 0.90]	0.84 [0.81, 0.87]	5.52 [4.58, 6.66]	0.16 [0.12, 0.21]
	Acuson	23	34.61 [23.12, 51.83]	0.92 [0.89, 0.94]	0.82 [0.78, 0.86]	0.88 [0.85, 0.91]	6.94 [5.32, 9.05]	0.20 [0.16, 0.26]
Max	Aixplorer	39	44.75 [29.08, 68.87]	0.93 [0.90, 0.95]	0.85 [0.82, 0.88]	0.89 [0.85, 0.92]	7.58 [5.65, 10.19]	0.17 [0.14, 0.21]
	Acuson	18	28.18 [19.48, 40.78]	0.91 [0.87, 0.93]	0.80 [0.75, 0.84]	0.87 [0.84, 0.91]	6.39 [4.88, 8.36]	0.23 [0.18, 0.28]
Min	Aixplorer	5	76.65 [6.98, 841.69]	0.94 [0.80, 1.04]	0.92 [0.66, 0.99]	0.86 [0.71, 0.94]	6.77 [2.77, 16.52]	0.09 [0.02, 0.50]
	Acuson	8	9.61 [6.33, 14.60]	0.82 [0.78, 0.86]	0.79 [0.64, 0.88]	0.72 [0.55, 0.84]	2.82 [1.88, 4.23]	0.29 [0.19, 0.44]
SD	Aixplorer	13	28.54 [18.52, 43.99]	0.89 [0.79, 0.96]	0.81 [0.78, 0.84]	0.87 [0.83, 0.90]	6.25 [4.61, 8.47]	0.22 [0.18, 0.26]
	Acuson	2	27.40 [6.60, 113.81]	0.91 [0.00, 1.31]	0.75 [0.41, 0.93]	0.90 [0.87, 0.93]	7.73 [4.95, 12.08]	0.28 [0.10, 0.82]

Many of the studies in the meta-analysis performed SWE using the Aixplorer SuperSonic Imagine system or the Siemens Acuson system. This subgroup analysis was performed to determine whether the machine used altered the overall analysis. Values are reported as mean [95 % CI]. AUC=area under the curve.

During data extraction, it was discovered that while most of the studies included in this meta-analysis only investigated lesions classified as BIRADS 3 or higher, several included patients with BIRADS 2 lesions (indicating benign categorization). To determine whether this discrepancy played a role in the overall results, an additional sub-group analysis was performed on studies that did not include BIRADS 2 lesions. As shown in Table 6, no significant difference between these results and those from the main analysis was identified.

Table 6: Sub-group Analysis – Studies evaluating only BIRADS 3+ lesions

	# Studies	DOR	AUC	Sensitivity	Specificity	LR+	LR-
Mean	57	40.00 [29.61, 54.04]	0.93 [0.91, 0.94]	0.86 [0.83, 0.88]	0.87 [0.85, 0.89]	6.55 [5.57, 7.71]	0.16 [0.13, 0.20]
Max	55	37.44 [27.81, 50.40]	0.92 [0.90, 0.94]	0.83 [0.80, 0.85]	0.88 [0.86, 0.90]	7.15 [5.85, 8.75]	0.19 [0.16, 0.22]
Min	12	27.14 [9.16, 80.43]	0.91 [0.82, 0.97]	0.84 [0.71, 0.92]	0.83 [0.74, 0.90]	5.09 [2.98, 8.67]	0.19 [0.09, 0.37]
SD	15	30.89 [18.52, 51.51]	0.91 [0.87, 0.94]	0.81 [0.75, 0.86]	0.88 [0.84, 0.91]	6.69 [4.89, 9.15]	0.22 [0.16, 0.29]

Most of the studies included in the meta-analysis evaluated lesions categorized as BIRADS 3 or above. However, several included BIRADS 2 cases. This subgroup analysis was performed to determine whether including BIRADS 2 lesions altered the overall analysis. Values are reported as mean [95 % CI]. AUC=area under the curve.

Utilization

Assuming that the estimated negative and positive LRs determined through this meta-analysis remain accurate across all of the initial BIRADS assessments, post-test probabilities were calculated and are presented for each SWE parameter in Tables 7-10.

Table 7: Probability of Malignancy Given Positive and Negative SWS_{Mean} Results

	Pre-Test	Post-Test (Negative)	Post-Test (Positive)
BIRADS 3	2.00 %	0.34 [0.28,0.41] %	11.51 [10.07,13.13] %
BIRADS 4a	10.00 %	1.81 [1.50,2.18] %	41.46 [37.86,45.15] %
BIRADS 4b	50.00 %	14.24 [12.07,16.71] %	86.44 [84.58,88.11] %
BIRADS 4c	95.00 %	75.93 [72.29,79.22] %	99.18 [99.05,99.29] %
BIRADS 5	100.00 %	100.00 [100.00,100.00] %	100.00 [100.00,100.00] %

Each row represents the upper limit of the probability of malignancy for each BIRADS category. This value is equal to the lower limit of the subsequent category. Probabilities based on likelihood ratios derived from studies utilizing the mean SWS are reported as mean [95 % CI]

Table 8: Probability of Malignancy Given Positive and Negative SWS_{Max} Results

	Pre-Test	Post-Test (Negative)	Post-Test (Positive)
BIRADS 3	2.00 %	0.40 [0.34,0.46] %	12.44 [10.42,14.79] %
BIRADS 4a	10.00 %	2.12 [1.83,2.46] %	43.62 [38.78,48.59] %
BIRADS 4b	50.00 %	16.30 [14.34,18.48] %	87.44 [85.08,89.48] %
BIRADS 4c	95.00 %	78.73 [76.08,81.16] %	99.25 [99.09,99.39] %
BIRADS 5	100.00 %	100.00 [100.00,100.00] %	100.00 [100.00,100.00] %

Each row represents the upper limit of the probability of malignancy for each BIRADS category. This value is equal to the lower limit of the subsequent category. Probabilities based on likelihood ratios derived from studies utilizing the maximum SWS are reported as mean [95 % CI]

Table 9: Probability of Malignancy Given Positive and Negative SWS_{Min} Results

	Pre-Test	Post-Test (Negative)	Post-Test (Positive)
BIRADS 3	2.00 %	0.36 [0.18,0.69] %	8.37 [5.14,13.34] %
BIRADS 4a	10.00 %	1.90 [0.99,3.64] %	33.21 [22.77,45.60] %
BIRADS 4b	50.00 %	14.86 [8.24,25.35] %	81.73 [72.63,88.30] %
BIRADS 4c	95.00 %	76.84 [63.03,86.58] %	98.84 [98.06,99.31] %
BIRADS 5	100.00 %	100.00 [100.00,100.00] %	100.00 [100.00,100.00] %

Each row represents the upper limit of the probability of malignancy for each BIRADS category. This value is equal to the lower limit of the subsequent category. Probabilities based on likelihood ratios derived from studies utilizing the minimum SWS are reported as mean [95 % CI]

Table 10: Probability of Malignancy Given Positive and Negative SWS_{SD} Results

	Pre-Test	Post-Test (Negative)	Post-Test (Positive)
BIRADS 3	2.00 %	0.42 [0.33,0.55] %	12.53 [9.58,16.23] %
BIRADS 4a	10.00 %	2.25 [1.74,2.90] %	43.82 [36.58,51.33] %
BIRADS 4b	50.00 %	17.16 [13.78,21.17] %	87.53 [83.85,90.47] %
BIRADS 4c	95.00 %	79.74 [75.22,83.62] %	99.26 [99.00,99.45] %
BIRADS 5	100.00 %	100.00 [100.00,100.00] %	100.00 [100.00,100.00] %

Each row represents the upper limit of the probability of malignancy for each BIRADS category. This value is equal to the lower limit of the subsequent category. Probabilities based on likelihood ratios derived from studies utilizing the standard deviation of the SWS are reported as mean [95 % CI]

For example, consider a BIRADS 4a lesion (pretest probability 2-10%) evaluated with the SWV_{min} parameter (Table 9). A SWV_{min} value that falls below the threshold constitutes a negative test and results in a post-test probability of 0.36-1.9%. This falls within the BI-RADS 3 pretest probability of 0-2%, indicating the lesion should be downgraded. Alternatively, a lesion initially classified as BI-RADS 3 with a SWS_{max} value (Table 8) above the cutoff would have a posttest probability of up to 12.44%, upgrading it to the BI-RADS 4A category.

Discussion

SWE is reproducible, quantitative, not operator dependent, and diagnostically accurate, as shown by the results of this analysis. In addition, the availability of

quantitative data in real time allows operators to adjust and optimize visualization of suspicious lesions [20]. Although SWE has been clinically available for decades, its use in the United States has been minimal. Just as the establishment of the BIRADs system was fundamental in driving the adoption of breast US, establishing guidelines for breast elastography may allow it to be similarly embraced by breast oncologists and radiologists alike.

Prior Work

Prior meta-analyses evaluating the diagnostic accuracy of SWE in evaluating suspicious breast lesions have produced results similar to those of this analysis. In 2013, Li et al. demonstrated the diagnostic accuracy of SSI, with a summary sensitivity and specificity of 0.91 (95% CI, 0.88-0.94) and 0.82 (95% CI, 0.75-0.87), and of ARFI imaging, with a summary sensitivity and specificity of 0.89 (95% CI, 0.81-0.94) and 0.91 (95% CI, 0.84-0.95), across 2,000 patients [49]. In 2014, Chen et al. analyzed 2,584 lesions using SWE and documented a sensitivity and specificity of 0.93 (95% CI, 0.91-0.95) and 0.81 (95% CI, 0.78-0.83) for maximum stiffness, 0.94 (95% CI, 0.92-0.96) and 0.71 (95% CI, 0.69-0.74) for mean stiffness, and 0.77 (95 % CI, 0.70-0.83) and 0.88 (95% CI, 0.84-0.91) for the standard deviation parameter [50]. Xue et al and Blank and Antaki focused solely on SWS_{mean} and SWS_{max}, bypassing SWS_{min} and SWS_{SD} [51, 52].

Li et al. and Liu et al. studied VTI and VTQ [53, 54]. Based off of their analysis, Liu et al proposed using a fixed-size ROI of 5 × 5 mm and a weighted SWS_{mean} cutoff value of 4.4 m/s in VTQ. Notably, this ROI differs from the majority of the ROI sizes used in this meta-analysis. Liu et al. were unable to determine summary statistics for

VTIQ due to insufficient data but estimated a sensitivity ranging from 80.4% to 90.3% and a specificity ranging from 73.0% to 93.0%. Luo et al. compared 2D and 3D SWE combined with B-mode US but did not explore the utility of 2D or 3D SWE alone [55].

SWE vs SE

The World Federation for Ultrasound in Medicine and Biology devised guidelines that define and discuss SE and SWE. However, they were unable to provide recommendations regarding the use of one technique over the other as, at the time, there were not enough studies comparing the two [56]. Thus, a secondary goal of this work was to facilitate this type of direct comparison by providing a systematic review and meta-analysis for SWE similar to those already available for SE.

For example, a SE meta-analysis performed by Barr et al. reported that the ratio of elastography to B-mode length was the most accurate SE technique, with a sensitivity of 96% (95% CI, 94%-98%) and specificity of 88% (95% CI, 85%-89%) out of three SE scoring systems [57]. It had a negative likelihood ratio of 0.03, suggesting SE can be used to downgrade BI-RADS 4A or 4B lesions (pretest probability of up to 50%) to BI-RADS 3 (<2% probability of malignancy).

The current meta-analysis demonstrated that SWE has a sensitivity of 86% (95% CI, 83%-88%) and a specificity of 87% (95% CI, of 84%-88%) using SWS_{mean} which is lower than that of SE. Additionally, while the results of the SE study showed its ability to downgrade BI-RADS 4B lesions to BI-RADS 3, per this study, while SWE can support downgrading lesions from BI-RADS 4A to BI-RADS 3, it cannot be used to completely exclude malignancy in a BI-RADS 4B lesion.

Thus, comparing these two similarly designed analyses reveals that the diagnostic performance of SWE lags behind that of SE. Two prospective studies published in 2020 and 2022 that compared SE and SWE directly further support this conclusion [58, 59]. Historically, one major challenge of SE was operator dependence and the steep learning curve faced by technicians learning how to apply optimal compression and release [56]. However, this no longer represents a primary concern as many modern systems utilize the patient's normal breathing motion rather than manual compression.

In contrast, SWE has two major limitations that have yet to be addressed. Precompression is the involuntary application of pressure by the transducer during measurement acquisition. This leads to elevated stiffness estimates due to nonlinear elastances and the generation of false-positives [60]. "Soft" or "blue" cancers are a type of artifact that can occur when scanning stiff breast lesions creates false-negative results, though this has been partially accounted for with the use of a quality or confidence map that confirms that the measured shear waves are adequate for estimating stiffness [61].

While SWE is not as effective in the evaluation of "soft" cancers, it performs well when evaluating benign lesions. Given that the sensitivity of SE is highest when characterizing malignant lesions, and the technique is less effective for benign lesions, using a combination of SE and SWE may produce an improved summary LR−, which could decrease the number of benign breast biopsies without affecting identification of malignant lesions. This theory was supported by a recent large multicenter trial which demonstrated that combining both modalities improved breast lesion characterization [62, 63].

Limitations

This meta-analysis had the following limitations. First, though previous studies have indicated a difference in the predictive abilities of 2-D SWE in Asian populations compared to White ones, our results were not controlled for age, ethnicity, or other demographic factors [51]. Also, the study of Lin et al. was an outlier, using a much larger sample size of 2,262 lesions [64]. Comparatively, the other 86 studies had an average study size of 212 ± 26 lesions (mean ± the standard error of the mean). Finally, because the approximate threshold values pooled over the included studies are dependent on the *weighted* average thresholds of these studies in HSROC analysis, definitive optimal SWS threshold values could not be determined. The best practice for identifying a definitive summary threshold would be to utilize the underlying data for each study included in the analysis, rather than the calculated results. It is also possible to introduce study level covariates to compare groups of studies which was not performed in this analysis.

Though HSROC analysis assumes the presence of study heterogeneity in included studies, there was substantial heterogeneity in the sensitivities and specificities reported. For example, some outlier studies demonstrated sensitivities as low as 50% for SWS_{mean} while a few small studies clustered near 100% sensitivity and specificity. The cause of this heterogeneity, visualized by the prediction ellipses and study scatter on the summary ROC in Figure 4, is unclear but may be partially explained by the lack of threshold standardization, as the retroactively calculated thresholds varied widely among the included studies [65]. The lack of standardization for the method of performing SWE, especially ROI selection may also play a role. Finally, the asymmetry displayed in the "funnel plots" can indicate publication bias, which could partially explain the clustering

of small, high-sensitivity and high-specificity studies. Therefore, since the smaller studies were more likely to be biased by random effects that tended toward higher sensitivity and specificity, it is possible that this analysis may overestimate the capabilities of SWE.

As stated previously, while the variance in ROI selection may be a potential confounder, most studies indicated that they placed the ROI over the stiffest portion of a mass. Per Moon et al., small ROIs placed at the stiffest area of the lesion were better at discriminating between benign and malignant tumors than large ROIs that covered the whole lesion [66]. Skerl et al. evaluated the influence of 1, 2, and 3 mm-sized ROIs on the discriminatory capacity of 2D SWE in solid breast lesions and discovered that the smallest ROI size resulted in the best diagnostic performance for the mean, but the SD parameter had the best diagnostic accuracy with an ROI size of 3 mm [67]. To avoid taking two sets of measurements when calculating the four SWS parameters, their recommendation was to use an ROI size of 2 mm as the diagnostic accuracy of E_{mean} and E_{SD} was almost as good with an ROI size of 1 mm vs 2 mm and an ROI size of 2 mm vs 3 mm, respectively.

All studies that met the eligibility criteria specified in the protocol were included in the meta-analysis regardless of the outcome of the QUADAS-2 assessment. For example, the study by Hong et al. did not indicate the impetus for SWE imaging in included patients, so applicability and lack of bias were both called into question [44]. Similarly, Elmoneam et al. did not provide a rationale for how the ROI was selected. Though ROI size and selection were not specified in the systematic review protocol, the wide variance of ROI sizes and the lack of clarity regarding ROI selection makes assessing whether they caused bias challenging [68].

Future Work

The results of this meta-analysis confirm the hypothesis that SWS_{mean}, SWS_{max}, SWS_{min}, and SWS_{SD} can characterize breast lesions with high specificity and sensitivity. Therefore, integrating SWE into current protocols for evaluating suspicious breast masses should be considered. However, as the performance of SWE does not appear to yet be on the same level as that of SE, incorporating elastography into standard diagnostic practices should not include SWE at the exclusion of SE. Rather, as the literature suggests that the strengths of each method may lie in characterizing different types of lesions, future studies should examine whether combining SE and SWE may prove synergistic to their diagnostic utility.

Determining a definitive optimal threshold value may be aided by the use of an alternative, nonstandard model for data pooling, such as those presented by Steinhauser et al. or by conducting a large, prospective trial, stratified by initial BI-RADS assessment, to test the cutoff parameters identified in this study [69].

Finally, though performing subgroup analyses by breast cancer subtype was beyond the scope of this analysis, it is integral as different cancer subtypes exhibit different levels of stiffness. In most solid tumors, desmoplastic reactions and neoplastic infiltration of interstitial tissue or the intraductal component cause an increase in density. Some malignant lesions may appear soft within an ROI with a surrounding margin demonstrating increased SWS that can help characterize it as malignant, while some lesions with increased stiffness on SWE may be benign due to additional fibrosis, such as hyalinized fibroadenomas, fibrosis and fat necrosis [27]. Fibrocystic disease also may

present with elevated density due to histological changes, though shear waves do not propagate in non-viscous fluids, like in a cyst [22]. Likewise, due to their composition, medullary, mucinous and papillary carcinomas and some infiltrating ductal carcinomas may not demonstrate increased stiffness [21]. Jebreel et al. also reported that small malignant lesions may not have the typical features associated with malignant carcinomas, such as fibrosis of the lesion stroma, edema, and a large variation in vascular diameter [70].

Additional Considerations

The assumptions made to facilitate elastography measurements ignore the challenges that arise when soft tissues are recognized as complex and heterogeneous, with both a viscous and an elastic mechanical response to compression. For example, heterogeneity can occur in the form of lesions with stiff elastic regions (due to fibrosis or calcifications) and soft viscous regions (due to blood pools and cystic degeneration areas) or lesions with mixed cystic and necrotic features [31]. The reflection of shear waves at structural tissue interfaces also opposes the assumption of homogeneity and can lead to incorrect estimates of SWS [21]. Moreover, fibroglandular tissue stiffness can vary up to 35% throughout the menstrual cycle which is an additional complexity that should be accounted for when analyzing SWE measurements [22].

Elastography calculations assume that biological tissue is incompressible; however, in reality, tissues may lose volume when compressed. Young's modulus of invasive carcinoma was shown to be 5 and 25 times larger than that of normal adipose tissue when precompression levels of 5% and 20% were applied, respectively, confirming

the nonlinear elastic behavior of biological tissues [21]. Finally, assuming that tissues are purely elastic neglects the presence of tissue viscosity which makes SWS, in part, dependent on the excitation frequency. As this frequency may vary across different vendors and techniques, the Quantitative Imaging Biomarkers Alliance is attempting to standardize measurements from different elastography techniques [31]. Therefore, widespread adoption of elastography to characterize breast lesions will likely require more complex modeling to account for viscoeleastic differences and tumor heterogeneity.

Dissemination

These findings were shared with the scientific community via publication online in the peer-reviewed Journal of the American College of Radiology in March of 2022 and in print in May 2022 [1]. Following publication, the article was designated as a continuing medical education article and questions were published alongside it to guide learning and comprehension.

This article was recognized on AuntMinnie.com, a forum for radiologists, business managers, technologists, and members of organized medicine to discuss the recent advances in medical imaging. Website personnel consist of executives, editors, and software engineers associated with the radiology industry [71].

Conclusion

The aim of this study was to assess the ability of SWE to differentiate benign and malignant breast lesions. This meta-analysis demonstrated no significant difference between SWS_{mean}, SWS_{max}, or SWS_{SD} in classifying lesions. SWE appears to be a

promising adjunct to mammography and US for breast cancer evaluation and has the potential to contribute to the early, non-invasive diagnosis of breast cancer. For example, through this meta-analysis, SWS_{mean} was shown to have a pooled sensitivity of 0.86 (95% CI, 0.83-0.88) and specificity of 0.87 (95% CI, 0.84-0.88) with a mean cutoff value ± SD of 3.89 ± 1.03 m/s. However, as an optimal threshold cannot be confirmed through HSROC analysis, a prospective trial is required to test and confirm these results.

Appendices

Appendix A: List of Included Studies

1. Ahmed AT. Diagnostic utility of strain and shear wave ultrasound elastography in differentiation of benign and malignant solid breast lesions. *Egyptian Journal of Radiology and Nuclear Medicine*. 2020;51(1).
2. Altintas YB, M.:Alabaz, O.:Celiktas, M. A qualitative and quantitative assessment of simultaneous strain, shear wave, and point shear wave elastography to distinguish malignant and benign breast lesions. *Acta Radiologica*. 2020.
3. Au FWF, Ghai S, Moshonov H, et al. Diagnostic performance of quantitative shear wave elastography in the evaluation of solid breast masses: Determination of the most discriminatory parameter. *Am. J. Roentgenol*. 2014;202(3):E328-E336.
4. Barr RG, Zhang Z. Shear-wave elastography of the breast: Value of a quality measure and comparison with strain elastography. *Radiology*. 2015;275(1):45-53.
5. Çebi Olgun D, Korkmazer B, Kılıç F, et al. Use of shear wave elastography to differentiate benign and malignant breast lesions. *Diagn Interv Radiol*. 2014;20(3):239-244.
6. Chang JM, Moon WK, Cho N, et al. Clinical application of shear wave elastography (SWE) in the diagnosis of benign and malignant breast diseases. *Breast Cancer Research and Treatment*. 2011;129(1):89-97.
7. Chang JM, Won JK, Lee KB, Park IA, Yi A, Moon WK. Comparison of shear-wave and strain ultrasound elastography in the differentiation of benign and malignant breast lesions. *Am. J. Roentgenol*. 2013;201(2):W347-W356.
8. Chen YP, Han T, Wu R, et al. Comparison of Virtual Touch Tissue Quantification and Virtual Touch Tissue Imaging Quantification for diagnosis of solid breast tumors of different sizes. *Clin Hemorheol Microcirc*. 2016;64(2):235-244.
9. Choi HJ, Ko KH, Jung HK. Shear Wave Elastography for Surgically Verified Breast Papillary Lesions: Is It Effective for Differentiation between Benign and Malignant Lesions. *J. Ultrasound Med*. 2017;36(10):2007-2014.

10. Choi HY, Seo M, Sohn YM, et al. Shear wave elastography for the diagnosis of small (<=2 cm) breast lesions: Added value and factors associated with false results. *Br. J. Radiol*. 2019;92(1097).

11. Choi HY, Sohn YM, Seo M. Comparison of 3D and 2D shear-wave elastography for differentiating benign and malignant breast masses: focus on the diagnostic performance. *Clin. Radiol*. 2017;72(10):878-886.

12. Cong R, Li J, Guo S. A new qualitative pattern classification of shear wave elastograghy for solid breast mass evaluation. *Eur. J. Radiol*. 2017;87:111-119.

13. Cong R, Li J, Wang X. Comparing Performance of Combinations of Shear Wave Elastography and B-Mode Ultrasound in Diagnosing Breast Masses: Is It Influenced by Mass Size? *Ultrasound Med. Biol*. 2017;43(10):2133-2143.

14. Dobruch-Sobczak K, Nowicki A. Role of Shear Wave Sonoelastography in Differentiation Between Focal Breast Lesions. *Ultrasound Med. Biol*. 2015;41(2):366-374.

15. Dong F, Wu H, Zhang L, et al. Diagnostic Performance of Multimodal Sound Touch Elastography for Differentiating Benign and Malignant Breast Masses. *J. Ultrasound Med*. 2019;38(8):2181-2190.

16. Dória MT, Jales RM, Conz L, Derchain SFM, Sarian LOZ. Diagnostic accuracy of shear wave elastography – Virtual touch ™ imaging quantification in the evaluation of breast masses: Impact on ultrasonography's specificity and its ultimate clinical benefit. *Eur. J. Radiol*. 2019;113:74-80.

17. Evans A, Whelehan P, Thomson K, et al. Differentiating benign from malignant solid breast masses: Value of shear wave elastography according to lesion stiffness combined with greyscale ultrasound according to BI-RADS classification. *Br. J. Cancer*. 2012;107(2):224-229.

18. Evans A, Whelehan P, Thomson K, et al. Quantitative shear wave ultrasound elastography: initial experience in solid breast masses. *Breast Cancer Research*. 2010;12(6):R104.

19. G A Elmoneam, Almolla RM, Ahmed AF, Ahmad Al Ekrashy M. Supersonic shear waves quantitative elastography and kinetic magnetic resonance dynamic curve in discriminating BI-RADS 4 breast masses: A comparative study. *Egyptian Journal of Radiology and Nuclear Medicine*. 2016;47(4):1773-1782.

20. Giannotti E, Vinnicombe S, Thomson K, et al. Shear-wave elastography and greyscale assessment of palpable probably benign masses: Is biopsy always required? *Br. J. Radiol*. 2016;89(1062).

21. Golatta M, Schweitzer-Martin M, Harcos A, et al. Evaluation of virtual touch tissue imaging quantification, a new shear wave velocity imaging method, for breast lesion assessment by ultrasound. *Biomed Res Int*. 2014;2014:960262.

22. Gu JP, E. C.:Ternifi, R.:Nayak, R.:Boughey, J. C.:Fazzio, R. T.:Fatemi, M.:Alizad, A. Individualized-thresholding Shear Wave Elastography combined with clinical factors improves specificity in discriminating breast masses. *Breast*. 2020;54:248-255.

23. Guruf A, Ozturk M, Bayrak IK, Polat AV. Shear wave versus strain elastography in the differentiation of benign and malignant breast lesions. *Turkish Journal of Medical Sciences*. 2019;49(5):1509-1517.

24. Han J, Li F, Peng C, et al. Reducing Unnecessary Biopsy of Breast Lesions: Preliminary Results with Combination of Strain and Shear-Wave Elastography. *Ultrasound Med. Biol*. 2019;45(9):2317-2327.

25. Hari S, Paul SB, Vidyasagar R, et al. Breast mass characterization using shear wave elastography and ultrasound. *Daign. Intervent. Imaging*. 2018;99(11):699-707.

26. Hong S, Woo OH, Shin HS, Hwang SY, Cho KR, Seo BK. Reproducibility and diagnostic performance of shear wave elastography in evaluating breast solid mass. *Clin. Imaging*. 2017;44:42-45.

27. Huang YN, Li F, Han J, et al. Shear Wave Elastography Of Breast Lesions: Quantitative Analysis Of Elastic Heterogeneity Improves Diagnostic Performance. *Ultrasound Med. Biol*. 2019;45(8):1909-1917.

28. Ianculescu V, Ciolovan LM, Dunant A, et al. Added value of Virtual Touch IQ shear wave elastography in the ultrasound assessment of breast lesions. *Eur J Radiol*. 2014;83(5):773-777.

29. Jiang HWY, X. D.:Zhang, L. N.:Song, L. X.:Gao, X. H. Diagnostic values of shear wave elastography and strain elastography for breast lesions. *Rev. Medica Chile*. 2020;148(9):1239-1245.

30. Kapetas P, Clauser P, Woitek R, et al. Virtual Touch IQ elastography reduces unnecessary breast biopsies by applying quantitative "rule-in" and "rule-out" threshold values. *Sci Rep*. 2018;8(1):3583.

31. Kapetas P, Woitek R, Clauser P, et al. A Simple Ultrasound Based Classification Algorithm Allows Differentiation of Benign from Malignant Breast Lesions by Using Only Quantitative Parameters. *Mol. Imaging Biol*. 2018;20(6):1053-1060.

32. Kim HJ, Kim SM, Kim B, et al. Comparison of strain and shear wave elastography for qualitative and quantitative assessment of breast masses in the same population. *Sci. Rep*. 2018;8(1):6197.

33. Kim HL, J.:Kang, B. J.:Kim, S. H. What shear wave elastography parameter best differentiates breast cancer and predicts its histologic aggressiveness? *Ultrasonography*. 2021;40(2):265-273.

34. Kim MY, Choi N, Yang JH, Yoo YB, Park KS. False positive or negative results of shear-wave elastography in differentiating benign from malignant breast masses: Analysis of clinical and ultrasonographic characteristics. *Acta Radiol*. 2015;56(10):1155-1162.

35. Kim S, Choi SH, Choi Y, Kook SH, Park HJ, Chung EC. Diagnostic performance of shear wave elastography of the breast according to scanning orientation. *J. Ultrasound Med*. 2014;33(10):1797-1804.

36. Kim SJ, Ko KH, Jung HK, Kim H. Shear wave elastography: Is it a valuable additive method to conventional ultrasound for the diagnosis of small (≥2 cm) breast cancer? *Medicine*. 2015;94(42):e1540.

37. Kong WT, Zhou WJ, Wang Y, Zhuang XM, Wu M. The value of virtual touch tissue imaging quantification in the differential diagnosis between benign and malignant breast lesions. *Journal of Medical Ultrasonics*. 2019;46(4):459-466.

38. Kong WTW, Y.:Zhou, W. J.:Zhang, Y. D.:Wang, W. P.:Zhuang, X. M.:Wu, M. Can measuring perilesional tissue stiffness and stiff rim sign improve the diagnostic performance between benign and malignant breast lesions? *Journal of Medical Ultrasonics*. 2021;48(1):53-61.

39. Lam MC, Wong KML, Mak WS, Kwok KMK, Lam HS, Wong CW. Breast sonoelastography: Our preliminary experience in 155 lesions. *Hong Kong Journal of Radiology*. 2016;19(4):287-292.

40. Lee BE, Chung J, Cha ES, Lee JE, Kim JH. Role of shear-wave elastography (SWE) in complex cystic and solid breast lesions in comparison with conventional ultrasound. *Eur. J. Radiol.* 2015;84(7):1236-1241.

41. Lee EJ, Jung HK, Ko KH, Lee JT, Yoon JH. Diagnostic performances of shear wave elastography: Which parameter to use in differential diagnosis of solid breast masses? *Eur. Radiol.* 2013;23(7):1803-1811.

42. Lee EJC, Y. W. Combination of Quantitative Parameters of Shear Wave Elastography and Superb Microvascular Imaging to Evaluate Breast Masses. *Korean Journal of Radiology.* 2020;21(9):1045-1054.

43. Lee SH, Chang JM, Kim WH, et al. Differentiation of benign from malignant solid breast masses: Comparison of two-dimensional and three-dimensional shear-wave elastography. *Eur. Radiol.* 2013;23(4):1015-1026.

44. Li DD, Xu HX, Guo LH, et al. Combination of two-dimensional shear wave elastography with ultrasound breast imaging reporting and data system in the diagnosis of breast lesions: a new method to increase the diagnostic performance. *Eur Radiol.* 2016;26(9):3290-3300.

45. Li DD, Xu HX, Liu BJ, Bo XW, Li XL, Wu R. Quality Measurement of Two-dimensional Shear Wave Speed Imaging for Breast Lesions: The Associated Factors and the Impact to Diagnostic Performance. *Sci. Rep.* 2017;7(1).

46. Li XL, Ren WW, Fu HJ, et al. Shear wave speed imaging of breast lesions: Speed within the lesion, fat-to-lesion speed ratio, or gland-to-lesion speed ratio? *Clin. Hemorheol. Microcirc.* 2017;67(1):81-90.

47. Li XL, Xu HX, Bo XW, et al. Value of Virtual Touch Tissue Imaging Quantification for Evaluation of Ultrasound Breast Imaging-Reporting and Data System Category 4 Lesions. *Ultrasound Med Biol.* 2016;42(9):2050-2057.

48. Lin X, Chang C, Wu C, et al. Confirmed value of shear wave elastography for ultrasound characterization of breast masses using a conservative approach in chinese women: A large-size prospective multicenter trial. *Cancer Management and Research.* 2018;10:4447-4458.

49. Liu H, Zhao LX, Xu G, et al. Diagnostic value of virtual touch tissue imaging quantification for benign and malignant breast lesions with different sizes. *Int. J. Clin. Exp. Med.* 2015;8(8):13118-13126.

50. Magalhaes M, Belo-Oliveira P, Casalta-Lopes J, et al. Diagnostic Value of ARFI (Acoustic Radiation Force Impulse) in Differentiating Benign From Malignant Breast Lesions. *Acad. Radiol.*;24(1):45-52.

51. Ng WL, Rahmat K, Fadzli F, et al. Shearwave elastography increases diagnostic accuracy in characterization of breast lesions. *Medicine*. 2016;95(12).

52. Park J, Woo OH, Shin HS, Cho KR, Seo BK, Kang EY. Diagnostic performance and color overlay pattern in shear wave elastography (SWE) for palpable breast mass. *Eur. J. Radiol.* 2015;84(10):1943-1948.

53. Ren WW, Li XL, He YP, et al. Two-dimensional shear wave elastography of breast lesions: Comparison of two different systems. *Clin. Hemorheol. Microcirc*. 2017;66(1):37-46.

54. Ren WW, Li XL, Wang D, Liu BJ, Zhao CK, Xu HX. Evaluation of shear wave elastography for differential diagnosis of breast lesions: A new qualitative analysis versus conventional quantitative analysis. *Clin. Hemorheol. Microcirc*. 2018;69(3):425-436.

55. Romeih MAEH, Ebeed AE, Sabry IM. Value of adding shear wave elastography to routine breast ultrasound examination in assessment of solid breast lesions. *Egyptian Journal of Radiology and Nuclear Medicine*. 2018;49(2):553-563.

56. Savas NY, Hale Colakoglu ER. The diagnostic value of virtual touch tissue imaging quantification shear wave elastography in differentiating benign and malignant breast masses. *Acta Med. Mediterr*. 2019;35(5):2567-2574.

57. Shang J, Ruan LT, Wang YY, et al. Utilizing size-based thresholds of stiffness gradient to reclassify BI-RADS category 3–4b lesions increases diagnostic performance. *Clin. Radiol.* 2019;74(4):306-313.

58. Shi XQ, Li JL, Wan WB, Huang Y. A set of shear wave elastography quantitative parameters combined with ultrasound bi-rads to assess benign and malignant breast lesions. *Ultrasound Med. Biol*. 2015;41(4):960-966.

59. Singla V, Prakash A, Prabhakar N, et al. Does Shear Wave Elastography Score Over Strain Elastography in Breast Masses or Vice Versa? *Current Problems in Diagnostic Radiology*. 2020;49(2):96-101.

60. Skerl K, Vinnicombe S, Giannotti E, Thomson K, Evans A. Influence of region of interest size and ultrasound lesion size on the performance of 2D shear wave elastography (SWE) in solid breast masses. *Clin. Radiol*. 2015;70(12):1421-1427.

61. Song EJ, Sohn YM, Seo M. Diagnostic performances of shear-wave elastography and B-mode ultrasound to differentiate benign and malignant breast lesions: the emphasis on the cutoff value of qualitative and quantitative parameters. *Clin. Imaging*. 2018;50:302-307.

62. Sravani NR, A.:Sureshkumar, S.:Vijayakumar, C.:Abdulbasith, K. M.:Balasubramanian, G.:Toi, P. C. Diagnostic role of shear wave elastography for differentiating benign and malignant breast masses. *South African Journal of Radiology*. 2021;24(1).

63. Sun JW, Wang XL, Zhao Q, et al. Virtual touch tissue imaging and quantification (VTIQ) in the evaluation of breast lesions: The associated factors leading to misdiagnosis. *Eur. J. Radiol*. 2019;110:97-104.

64. Suvannarerg V, Chitchumnong P, Apiwat W, et al. Diagnostic performance of qualitative and quantitative shear wave elastography in differentiating malignant from benign breast masses, and association with the histological prognostic factors. *Quantitative Imaging in Medicine and Surgery*. 2019;9(3):386-398.

65. T. Klotz VB, F. Kwiatkowski, V. Dieu-de Fraissinette, A. Bailly-Glatre, S. Lemery and L. Boyer. Shear wave elastography contribution in ultrasound diagnosis management of breast lesions. *Daign. Intervent. Imaging*. 2014;95(9):813-824.

66. Tang F, Kang YF, Lu GL, et al. A comparative study of three ultrasonic elastographic methods for the differentiation and diagnosis of benign and malignant breast masses. *Clin. Exp. Obstet. Gynecol*. 2019;46(4):587-592.

67. Tang L, Xu HX, Bo XW, et al. A novel two-dimensional quantitative shear wave elastography for differentiating malignant from benign breast lesions. *Int. J. Clin. Exp. Med*. 2015;8(7):10920-10928.

68. Tian J, Liu Q, Wang X, Xing P, Yang Z, Wu C. Application of 3D and 2D quantitative shear wave elastography (SWE) to differentiate between benign and malignant breast masses. *Sci. Rep.* 2017;7.

69. Tozaki M, Saito M, Benson J, Fan L, Isobe S. Shear Wave Velocity Measurements for Differential Diagnosis of Solid Breast Masses: A Comparison between Virtual Touch Quantification and Virtual Touch IQ. *Ultrasound Med. Biol.* 2013;39(12):2233-2245.

70. Uysal EO, M.:Kilincer, A.:Koplay, M. Comparison of the Effectiveness of Shear Wave Elastography and Superb Microvascular Imaging in the Evaluation of Breast Masses. *Ultrasound Q.* 2021;37(2):191-197.

71. Wang B, Cai Z, Hu Y, et al. The differential diagnosis of benign and malignant breast cancer using shear wave elastography (SWE). *Biomed. Res.* 2017;28(17):7404-7411.

72. Wang Q, Li XL, He YP, et al. Three-dimensional shear wave elastography for differentiation of breast lesions: An initial study with quantitative analysis using three orthogonal planes. *Clin. Hemorheol. Microcirc.* 2019;71(3):311-324.

73. Wang YL, Y.:Zheng, X.:Huang, Y.:Han, J.:Li, F.:Mao, R.:Li, Q.:Cao, L.:Zhou, J. Added Value of Different Types of Elastography in Evaluating Ultrasonography Detected Breast Lesions: A Compared Study With Mammography. *Clin. Breast Cancer.* 2020;20(3):e366-e372.

74. Wang ZL, Li JL, Li M, Huang Y, Wan WB, Tang J. Study of quantitative elastography with supersonic shear imaging in the diagnosis of breast tumours. *La Radiologia medica.* 2013;118(4):583-590.

75. Wang ZL, Sun L, Li Y, Li N. Relationship between elasticity and collagen fiber content in breast disease: A preliminary report. *Ultrasonics.* 2015;57(C):44-49.

76. Xiang LH, Yao MH, Xu G, et al. Diagnostic value of contrast-enhanced ultrasound and shear-wave elastography for breast lesions of sub-centimeter. *Clin. Hemorheol. Microcirc.* 2017;67(1):69-80.

77. Yang P, Peng Y, Zhao H, Luo H, Jin Y, He Y. Can continuous scans in orthogonal planes improve diagnostic performance of shear wave elastography for breast lesions? *Technology and Health Care.* 2015;23(Supplement 2):S293-S300.

78. Yang Y-P, Xu X-H, Guo L-H, et al. Qualitative and quantitative analysis with a novel shear wave speed imaging for differential diagnosis of breast lesions. *Sci. Rep*. 2017;7(1):40964.

79. Yoon JH, Jung HK, Lee JT, Ko KH. Shear-wave elastography in the diagnosis of solid breast masses: What leads to false-negative or false-positive results? *Eur. Radiol*. 2013;23(9):2432-2440.

80. Yoon JH, Ko KH, Jung HK, Lee JT. Qualitative pattern classification of shear wave elastography forbreast masses: How it correlates to quantitative measurements. *Eur. J. Radiol*. 2013;82(12):2199-2204.

81. Youk JH, Son EJ, Gweon HM, Kim H, Park YJ, Kim JA. Comparison of strain and shear wave elastography for the differentiation of benign from malignant breast lesions, combined with b-mode ultrasonography: Qualitative and quantitative assessments. *Ultrasound Med. Biol*. 2014;40(10):2336-2344.

82. Zhang Q, Xiao Y, Chen S, Wang C, Zheng H. Quantification of Elastic Heterogeneity Using Contourlet-Based Texture Analysis in Shear-Wave Elastography for Breast Tumor Classification. *Ultrasound in Medicine & Biology*. 2015;41(2):588-600.

83. Zhang SP, Zeng Z, Liu H, Yao MH, Xu G, Wu R. Combination of conventional ultrasonography and virtual touch tissue imaging quantification for differential diagnosis of breast lesions smaller than 10mm. *Clin. Hemorheol. Microcirc*. 2017;67(1):59-68.

84. Zhang Y, Zhao CK, Li XL, et al. Virtual touch tissue imaging and quantification: value in malignancy prediction for complex cystic and solid breast lesions. *Sci. Rep*. 2017;7(1):7807.

85. Zheng X, Huang Y, Liu Y, et al. Shear-wave elastography of the breast: Added value of a quality map in diagnosis and prediction of the biological characteristics of breast cancer. *Korean Journal of Radiology*. 2020;21(2):172-180.

86. Zhou J, Zhan W, Chang C, et al. Breast Lesions: Evaluation with Shear Wave Elastography, with Special Emphasis on the "Stiff Rim" Sign. *Radiology*. 2014;272(1):63-72.

87. Zhu YJ, X. H.:Zhou, W.:Zhan, W. W.:Zhou, J. Q. Qualitative evaluation of virtual touch imaging quantification: A simple and useful method in the diagnosis of breast lesions. *Cancer Management and Research*. 2020;12:2037-2045.

Appendix B: Characteristics of Included Studies

Study # refers to the number assigned to each study in Appendix A.

Study #	Study Dates	# of Patients	# of Lesions	Average Age	BIRADS Categories	Reference Standard	Imaging System
1	2018-2019	100	132	42.4	1, 2, 3, 4, 5, 6	FNA, Core Biopsy, or Surgical Excision	GE Logic P9
2	2019-2020	159	163	45.5	3,4,5	Core Biopsy	Mindray Resona 7
3	2011-2012	112	123	49.2	3, 4, 5	US follow-up or Core Biopsy	Supersonic Imagine Aixplorer
4	2011-2012	143	165	48.5	1, 2, 3, 4, 5	FNA, Core Biopsy, or Surgical Excision	Siemens Acuson S2000
5	2012	109	115	51.0	3, 4, 5	Core Biopsy	Supersonic Imagine Aixplorer
6	2010	158	182	48.1	3, 4, 5	Core Biopsy or Surgical Excision	Supersonic Imagine Aixplorer
7	2010	129	150	47.8	3, 4, 5	US follow-up, Core Biopsy, or Surgical Excision	Supersonic Imagine Aixplorer
8	2014-2015	230	246	45.8	Not Specified	Core Biopsy or Surgical Excision	Siemens Acuson S3000
9	2012-2015	54	56	40.8	3, 4	US follow-up, Core Biopsy, or Surgical Excision	Supersonic Imagine Aixplorer

10	2013-2017	415	428	49.5	2, 3, 4, 5	Core Biopsy or Surgical Excision	Supersonic Imagine Aixplorer
11	2014-2016	199	205	51.7	3, 4, 5	Core Biopsy or Surgical Excision	Supersonic Imagine Aixplorer
12	2015-2016	314	325	44.6	3, 4, 5	Core Biopsy or Surgical Excision	Supersonic Imagine Aixplorer
13	2015-2016	315	326	44.5	3, 4, 5	Core Biopsy or Surgical Excision	Supersonic Imagine Aixplorer
14	Unspecified	76	84	53.9	3, 4, 5	FNA or Core Biopsy	Supersonic Imagine Aixplorer
15	2016-2017	159	159	40.4	3, 4, 5	Core Biopsy or Surgical Excision	Mindray Resona 7
16	2016-2017	357	396	54.2	3, 4, 5	2-year stability or Core Biopsy	Siemens Acuson S2000
17	2010	173	175	56.0	2, 3, 4, 5	Core Biopsy or Surgical Excision	Supersonic Imagine Aixplorer
18	Unspecified	52	53	53.0	2, 3, 4, 5	Core Biopsy or Surgical Excision	Supersonic Imagine Aixplorer
19	2014-2015	63	63	34.7	4	Core Biopsy or Surgical Excision	Not Specified

20	2010-2014	682	694	56.0	3, 4, 5	Core Biopsy or Surgical Excision	Supersonic Imagine Aixplorer
21	2012	103	104	51.0	3, 4,5	Core Biopsy	Siemens Acuson S3000
22	2020	644	659	54.4	4,5	FNA or Core Biopsy	GE Logic P9
23	2015	84	87	49.6	3, 4, 5	Core Biopsy	Siemens Acuson S2000
24	2016-2017	267	278	44.7	4	Core Biopsy	Siemens Acuson S2000
25	2013-2014	119	119	42.3	3, 4	Core Biopsy	Supersonic Imagine Aixplorer
26	2014-2015	218	264	46.4	3,4,5	Core Biopsy or Surgical Excision	Not Specified
27	2016-2017	267	278	45.6	3, 4, 5	US Follow-up, Core Biopsy, or Surgical Excision	Siemens Acuson S2000
28	2012	110	110	Not Specified	2, 3, 4, 5	FNA or Core Biopsy	Siemens Acuson S3000
29	2017-2018	132	164	44.6	3, 4, 5	Core Biopsy or Surgical Excision	Supersonic Imagine Aixplorer
30	2013-2015	189	196	Not Specified	2, 3, 4, 5	US follow-up or Core Biopsy	Siemens Acuson S3000

31	2015-2016	124	124	52.0	4, 5	Core Biopsy	Siemens Acuson S3000
32	2015	94	108	48.7	4, 5	US follow-up or Core Biopsy	Supersonic Imagine Aixplorer
33	2018-2019	190	211	48.0	3,4,5	Core Biopsy or Surgical Excision	Toshiba Aplio i700
34	2013	164	166	45.3	3, 4, 5	Core Biopsy	Supersonic Imagine Aixplorer
35	2012	235	260	44.0	Not Specified	Core Biopsy or Surgical Excision	Supersonic Imagine Aixplorer
36	2012-2013	171	177	45.2	3, 4, 5	Core Biopsy	Supersonic Imagine Aixplorer
37	2015-2018	454	466	41.6	3, 4, 5	US Core Biopsy, Tomographic Biopsy, or Surgical Excision	Siemens Acuson S3000
38	2017-2019	192	199	44.6	3,4,5	US Core Biopsy, Tomographic Biopsy, or Surgical Excision	Mindray Resona 7
39	2014-2015	155*	88	51.3	3, 4, 5	Histology acquired, unclear method	Siemens Acuson S3000
40	2013	139	140	45.5	4, 5	Core Biopsy	Supersonic Imagine Aixplorer

41	2012	139	156	43.5	3, 4, 5	Core Biopsy	Supersonic Imagine Aixplorer
42	2018-2019	192	200	49.0	3,4,5	Core Biopsy	Toshiba Aplio i800
43	2011	134	144	49.1	3, 4, 5	Core Biopsy or Surgical Excision	Supersonic Imagine Aixplorer
44	2014	276	296	45.4	2, 3, 4, 5	Core Biopsy or Surgical Excision	Siemens Acuson S3000
45	2014-2015	338	361	45.0	Not Specified	Core Biopsy or Surgical Excision	Siemens Acuson S3000
46	2016	182	182	45.9	3, 4, 5	Core Biopsy or Surgical Excision	Toshiba Aplio 500
47	2014-2015	116	116	48.5	4	Core Biopsy or Surgical Excision	Siemens Acuson S3000
48	2014-2015	2262	2262	43.0	2, 3, 4, 5	US follow-up, FNA, Core Biopsy, or Surgical Excision	Supersonic Imagine Aixplorer
49	2014	130	139	44.7	Not Specified	Core Biopsy or Surgical Excision	Siemens Acuson S3000
50	2013	81	92	50.0	3, 4, 5	Core Biopsy or Surgical Excision	Siemens Acuson S3000
51	2012-2013	152	159	52.0	3, 4, 5	Core Biopsy or Surgical Excision	Supersonic Imagine Aixplorer

52	2013-2014	133	156	47.8	4, 5	US follow-up, Core Biopsy, or Surgical Excision	Supersonic Imagine Aixplorer
53	2016	153	153	46.4	Not Specified	Core Biopsy or Surgical Excision	Toshiba Aplio 500
54	2014-2016	266	266	44.6	Not Specified	Core Biopsy or Surgical Excision	Siemens Acuson S3000
55	2016-2017	150	150	Not Specified	3, 4, 5	Core Biopsy or Surgical Excision	Toshiba Aplio
56	2017	63	63	47.8	3, 4, 5	Core Biopsy	Siemens Acuson S2000
57	2016-2017	222	234	44.2	3, 4, 5	Core Biopsy	Supersonic Imagine Aixplorer
58	2011-2013	251	279	45.3	3, 4, 5	Core Biopsy or Surgical Excision	Supersonic Imagine Aixplorer
59	2015-2016	192	199	Not Specified	2, 3, 4, 5	Core Biopsy or Surgical Excision	Supersonic Imagine Aixplorer
60	2012-2013	206	210	57.9	4, 5	Core Biopsy or Surgical Excision	Supersonic Imagine Aixplorer
61	2013-2015	198	209	47.0	3, 4, 5	Core Biopsy or Surgical Excision	Supersonic Imagine Aixplorer

62	2015-2017	163	175	Not Specified	Not Specified	Core Biopsy or Surgical Excision	Siemens Acuson S3000
63	2017-2018	237	252	43.2	3, 4, 5	Core Biopsy or Surgical Excision	Siemens Acuson S3000
64	2016-2017	228	244	51.3	4, 5	Core Biopsy	Supersonic Imagine Aixplorer
65	2012	142	167	57.7	3, 4, 5	Core Biopsy	Supersonic Imagine Aixplorer
66	2014-2015	97	97	46.7	Not Specified	Surgical (Mastectomy)	Not Specified
67	2014	98	133	43.8	2, 3, 4, 5	Core Biopsy or Surgical Excision	Siemens Acuson S3000
68	2014-2015	210	210	43.1	2, 3, 4, 5	Core Biopsy	Supersonic Imagine Aixplorer
69	2012	81	83	49.0	4, 5	US follow-up or Core Biopsy	Siemens Acuson S3000
70	2019	121	121	50.5	4,5	Core Biopsy	Toshiba Aplio 500
71	2013-2016	63	63	Not Specified	3, 4, 5	Core Biopsy or Surgical Excision	Supersonic Imagine Aixplorer

72	2016-2017	122	122	45.0	3, 4, 5	Core Biopsy or Surgical Excision	Supersonic Imagine Aixplorer
73	2016-2018	289	316	46.6	3,4,5	US follow-up, Core Biopsy, or surgical excision	Siemens Acuson S2000
74	2010	108	114	42.8	3, 4, 5	Core Biopsy	Supersonic Imagine Aixplorer
75	2012-2013	106	116	51.8	Not Specified	Core Biopsy	Supersonic Imagine Aixplorer
76	2015-2016	62	66	49.3	3, 4	Core Biopsy or Surgical Excision	Supersonic Imagine Aixplorer
77	2014-2015	119	122	Not Specified	Not Specified	Core Biopsy	Supersonic Imagine Aixplorer
78	2016	218	225	45.3	Not Specified	Core Biopsy or Surgical Excision	Toshiba Aplio 500
79	2012	199	222	45.3	3, 4, 5	Core Biopsy or Surgical Excision	Supersonic Imagine Aixplorer
80	2012-2013	236	267	45.1	3, 4, 5	Core Biopsy or Surgical Excision	Supersonic Imagine Aixplorer

81	2012	78	79	45.5	3, 4, 5	Core Biopsy	Supersonic Imagine Aixplorer
82	2012-2013	125	161	40.4	Not Specified	Core Biopsy or Surgical Excision	Supersonic Imagine Aixplorer
83	2014	97	98	44.7	Not Specified	FNA or Surgical Excision	Siemens Acuson S3000
84	2014-2015	89	89	45.4	3, 4, 5	Core Biopsy	Siemens Acuson S3000
85	2016-2019	368	368	47.0	4, 5	Core Biopsy	Siemens Acuson S2000
86	2011	193	193	46.0	3, 4,5	Core Biopsy	Supersonic Imagine Aixplorer
87	2016-2017	230	230	44.7	3,4,5	Core Biopsy	Siemens Acuson S3000

* Study 39 provided the initial study size but not the total number of patients included in the final analysis.

Appendix C: QUADAS-2 Assessments of Bias and Applicability for Included Studies

Study # refers to the number assigned to each study in Appendix A.

☺ - Low Risk/Concern, ☹ - High Risk/Concern, ? - Unclear Risk/Concern

Study #	Risk of Bias				Applicability Concerns		
	Patient Selection	Index Test	Reference Standard	Flow and Timing	Patient Selection	Index Test	Reference Standard
1	☺	☺	☺	☺	☺	☺	☺
2	☺	☺	☺	☺	☺	☺	☺
3	☺	☺	☺	☺	☺	☺	☺
4	☺	☺	☺	☺	☺	☺	☺
5	☺	☺	☺	☺	☺	☺	☺
6	☺	☺	☺	☺	☺	☺	☺
7	☺	☺	☺	☺	☺	☺	☺
8	☺	☺	☺	☺	☺	☺	☺
9	☺	☺	☺	☺	☺	☺	☺
10	☺	☺	☺	☺	☺	☺	☺
11	☺	☺	☺	☺	☺	☺	☺
12	☺	☺	☺	☺	☺	☺	☺
13	☺	☺	☺	☺	☺	☺	☺
14	?	☺	☺	?	?	☺	☺
15	☺	☺	☺	☺	☺	☺	☺
16	☺	☺	☺	☺	☺	☺	☺
17	☺	☺	☺	☺	☺	☺	☺
18	☺	☺	☺	☺	☺	☺	☺
19	?	?	☺	☺	?	☺	☺

20	☺	☺	☺	☺	☹	☺	☺
21	☺	☺	☺	☺	☺	☺	☺
22	☺	☺	☺	☺	☺	☺	☺
23	☺	☺	☺	☺	☺	☺	☺
24	☺	☺	☺	☺	?	☺	☺
25	☺	☺	☺	☺	☺	☺	☺
26	☹	☺	☺	☺	☹	☺	☺
27	☺	☺	?	☺	☺	?	☺
28	☺	☺	☺	☺	☺	☺	☺
29	☺	☺	☺	☺	☺	☺	☺
30	?	☺	☺	☺	☹	☺	☺
31	☺	☺	☺	☺	☺	☺	☺
32	☺	☺	☺	☹	☺	☺	☺
33	☹	☺	☺	?	☺	☺	☺
34	☺	☺	☺	?	☺	☺	☺
35	☺	☺	☺	☺	☺	☺	☺
36	?	☺	☺	?	?	☺	☺
37	☺	☺	☺	☺	☺	☺	☺
38	?	☹	☺	☺	☺	☺	☺
39	☺	☺	?	?	☺	☺	?
40	?	☺	☺	?	?	☺	☺
41	☺	☺	☺	?	☺	☺	☺
42	☺	☺	☺	☺	☺	☺	☺
43	☺	☺	☺	☺	☺	☺	☺
44	☺	☺	☺	?	☺	☺	☺

45	☺	☺	☺	☺	☺	☺	☺
46	☺	☺	☺	☺	☺	☺	☺
47	☺	☺	☺	☺	☺	☺	☺
48	☺	☺	☺	☺	☺	☺	☺
49	☺	☺	☺	☺	☺	☺	☺
50	☺	☺	☺	☺	☺	☺	☺
51	☺	?	☺	☺	☺	☺	☺
52	☺	☺	☺	☺	☺	☺	☺
53	☺	☺	☺	☺	☺	☺	☺
54	☺	☺	☺	☺	☺	☺	☺
55	☺	☺	☺	☺	☺	☺	☺
56	☺	☺	☺	☺	☺	☺	☺
57	☺	☺	☺	☺	☺	☺	☺
58	☺	☺	☺	☺	☺	☺	☺
59	☺	☺	☺	☺	☺	☺	☺
60	☺	☺	☺	☺	☺	☺	☺
61	?	☺	☺	☺	☺	☺	☺
62	☹	☺	☺	☺	☹	☺	☺
63	?	?	☺	☺	☺	☺	☺
64	☺	☺	☺	☺	☺	☺	☺
65	?	☺	☺	☺	☺	☺	☺
66	?	?	☺	☺	☺	☺	☺
67	☺	☺	☺	☺	☺	☺	☺
68	☺	☺	☺	☺	☺	☺	☺
69	☺	☺	☺	☺	☺	☺	☺

70	☺	☺	☺	☺	☺	☺	☺
71	☺	☺	☺	☺	☺	☺	☺
72	☺	☺	☺	☺	☺	☺	☺
73	?	☺	☺	☺	?	☺	☺
74	☺	☺	☺	☺	☺	☺	☺
75	☺	☺	☺	☺	☺	☺	☺
76	☺	☺	☺	☺	☺	☺	☺
77	☺	☺	☺	☺	☺	☺	☺
78	☺	☺	☺	☺	☺	☺	☺
79	☺	☺	☺	?	☺	☺	☺
80	☺	☺	☺	?	☺	☺	☺
81	☺	☺	☺	☺	☺	☺	☺
82	☺	☺	☺	☺	☺	☺	☺
83	☺	☺	☺	☺	☺	☺	☺
84	☹	?	☺	☺	☹	☺	☺
85	?	?	☺	☺	?	☺	☺
86	☺	☺	☺	☺	☺	☺	☺
87	☺	☺	☺	☺	☺	☺	☺
☺	71	80	85	76	75	86	86
☹	4	1	0	1	5	0	0
?	12	6	2	10	7	1	1

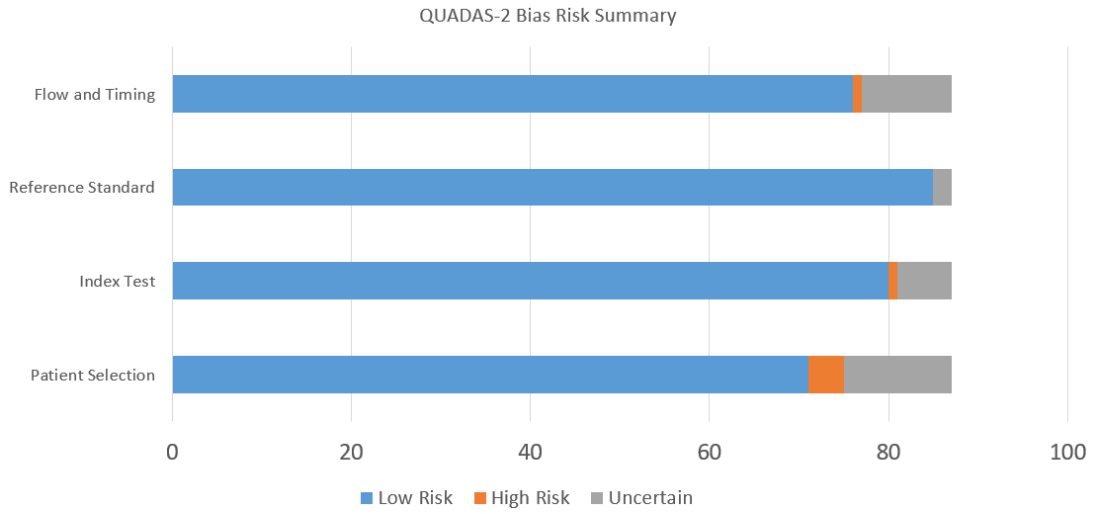

Figure C1. Most of the included studies were well-suited to the study protocol which decreased the risk that their inclusion would bias the results. However, multiple studies did contain variations or incomplete information that created uncertainty or increased the risk of bias.

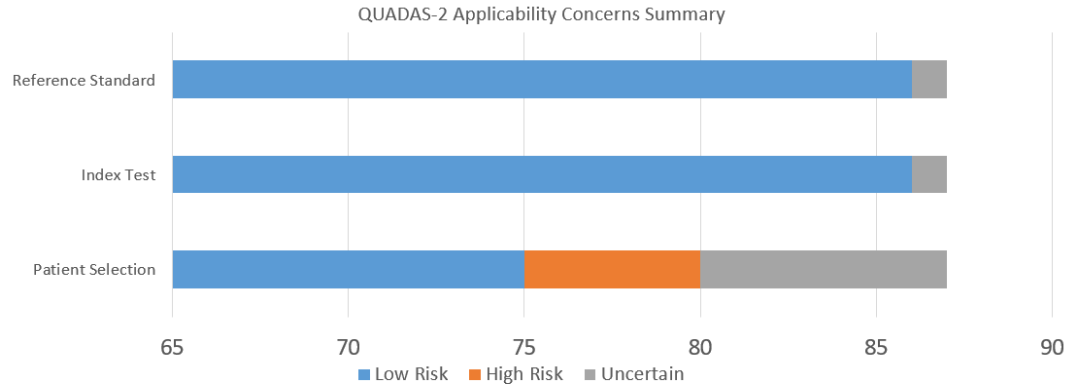

Figure C2. All the included studies met the eligibility criteria for this systematic review, utilizing consistent reference standards (biopsy or 2-year stability) and index tests (2D SWE). However, several studies did not fully outline the criteria used for patient selection which raised concerns of applicability.

Appendix D: Study Protocol

Citation: Pillai, A., Voruganti, T., Barr, R., & Langdon, J. Diagnostic Accuracy of Shear Wave Elastography for Breast Lesion Characterization in Women: A Systematic Review and Meta-Analysis. Open Science Framework 2021.

Review Question: What is the diagnostic performance (sensitivity and specificity) of 2D Shear Wave Elastography (2D-SWE) in the differentiation of benign and malignant breast lesions with respect to the mean, minimum, maximum, and standard deviation of the intra-lesional shear wave speed?

Aim 1: To synthesize the existing data on shear wave elastography in order to determine a cutoff threshold for the identification of malignant breast lesions in women.

Aim 2: To assess the impact of the shear wave velocity parameters and thresholds utilized on corresponding sensitivity and specificity values.

Searches:

A systematic search of the medical literature will be performed using PubMed, Scopus, Embase, Ovid-Medline, The Cochrane Library and Web of Science.

The search will employ sensitive topic-based strategies designed for each database from inception to published prior to June 21, 2021. Papers in English or with an English translation available will be considered. There will be no geographical restrictions.

Search terms will be generated based on key articles identified. The search will be by MeSH terms as well as search terms mentioned anywhere in the article. The bibliography of key articles will also be searched.

The following major terms will be applied: “breast neoplasm,” “elasticity imaging,” “shear wave elastography,” “mammary ultrasound,” “breast ultrasound,” “virtual touch tissue imaging quantification,” “breast tumor,” “echography,” “elastography,” “VTIQ,” and “ultrasound.”

Duplicates will be eliminated from the search results, and the references of the remaining articles will be screened for any further relevant material.

Type of study to be included:

Study designs included will be diagnostic measure studies evaluating diagnostic accuracy with at least 50 cases. Papers identified as review articles, case reports, letters and editorials, and studies that included clinically selected study populations will be excluded. Discrepancies will be resolved by consensus between AP and TV. If agreement cannot be reached, a third reviewer (JL) will be consulted, and the majority opinion will be used for analysis. Appropriate abstracts with sufficient information will be included.

Design and methods used for this systematic review are reported in line with Preferred Reporting Items for Systematic Reviews and Meta-Analyses – Diagnostic Test Accuracy (PRISMA-DTA).

Condition or domain being studied: Benign and malignant breast lesions

Participants/Population: Women with breast lesions with no prior treatment or history of breast augmentation who need to undergo further workup.

Intervention(s), exposure(s): Two-dimensional shear wave elastography (SWE, ARFI).

Comparator(s)/control: Biopsy or surgery-proven cases or stability of lesion over two years (i.e. benign).

Main outcome(s):

1) Shear wave velocity, shear modulus, or Young's modulus cut-off value determined retroactively
2) Associated diagnostic accuracy values (sensitivity and specificity or the data required to calculate them)

Data extraction (selection and coding):

All references identified by our search strategy will be independently assessed by two authors, first by title and abstract, then by review of the complete paper. The full texts of papers identified as being potentially relevant for inclusion will then be reviewed, and additional articles will be obtained through a screening of the reference lists. Studies will be eligible for inclusion if they fulfilled the following criteria:

1. Include patients with the gold standard for diagnosis, namely biopsy-proven diagnosis or 2-year stability of the lesion.

2. Present the results in terms of either in terms of the measured shear wave velocity or shear modulus or provided data allowing for their calculation. The study must describe thresholds used on these parameters for determination of benignity or malignancy.
3. Include at least fifty cases.
4. Described the statistics and thresholds used on these parameters for determination of benignity or malignancy, including utilizing the mean, minimum, maximum, or standard deviation over the described region of interest

Review articles, case reports, letters, and editorials will be excluded. Discrepancies will be resolved by consensus, and if agreement cannot be reached, a third reviewer will be consulted, and the majority opinion followed.

For each article, study design, year of publication, bibliographic data, number of patients, mean age, age range, type of lesion, and range of lesion diameter, prevalence of malignant lesions, SWS, Shear Modulus, or Young's Modulus threshold values, cut-off value, region of interest (ROI), and the diagnostic sensitivity and specificity of 2D-SWE will be collected.

Risk of bias (quality) assessment:

The QUADAS-2 checklist will be used for quality assessment.

The possibility of publication bias will be assessed using a funnel plot analysis and a trim-and-fill analysis to identify "missing studies," as well as the Rank Correlation test.

Strategy for data synthesis:

Sensitivity and specificity will be pooled with weighted averages applied, in which the weight of each study will be its sample size. As no diagnostic threshold exists for histological diagnoses, a hierarchical summary receiver operating characteristic curve, introduced by Rutter et al. will be constructed.

Study heterogeneity will be assessed using the I^2 index, which describes the percentage of total variation across studies which is due to heterogeneity rather than to chance, and a value of >50% may be considered to be indicative of significant heterogeneity. If the presence of heterogeneity is demonstrated,

subgroup analysis will be performed according to the common methodological and clinical features of the studies, to identify the possible sources of the heterogeneity.

Analysis of subgroups or subsets:

1) Analysis between different vendors of shear wave elastography technology and devices (Aixplorer vs. Acuson).
2) Analysis between studies examining BI-RADS 3, 4, and 5 lesions only versus studies that include BI-RADS 2 lesions in addition to 3, 4, and 5.

Contact for further information: jonathan.langdon@yale.edu

Organizational affiliation of the review: None

Review team members and their organizational affiliations:

Aishwarya Pillai[1], Teja Voruganti[1], Richard Barr[2], and Jonathan Langdon[1]. [1]Department of Radiology, Yale University School of Medicine, New Haven, CT. [2]Department of Radiology, Northeastern Ohio Medical University, Rootstown, OH

Type and method of review: Systematic review with meta-analysis and subgroup analysis

Anticipated or actual start date: April 4th, 2020

Anticipated completion date: June 30, 2021

Funding sources/sponsors: Funding has been provided by the Yale Medical Student Fellowship.

Conflicts of Interest: None known

Language: English

Country: Unites States of America

Stage of review: Review in progress

Stage	**Started**	**Completed**
Preliminary searched	Yes	Yes
Piloting of the study selection process	Yes	Yes
Formal screening of search results against eligibility criteria	Yes	Yes

Data extraction	Yes	Yes
Risk of bias (quality) assessment	Yes	Yes
Data analysis	Yes	Yes

This protocol is an update of a previous protocol published November 28, 2020 at doi:10.17605/OSF.IO/7Z8EM amended June 14, 2021 with the following changes:

1) Title updated.
2) "Aim 1" and "Aim 2" added for clarification.
3) Search term "breast ultrasound" added to avoid limiting results by only using "mammary ultrasound"
4) Search end date updated to June 21st, 2021
5) Reviewer initials added in "Type of study to be included" for clarity.
6) Wording updated to reflect that the design and methods used are in line with PRISMA-DTA.
7) VTIQ removed from eligibility criteria
8) "Diagnostic yield" and "diagnostic odds ratio" removed as a main outcome.
9) Main outcomes separated and listed
10) "Shear wave velocity, shear modulus, or Young's modulus cut-off value" added as a main outcome
11) "long term stability of the lesion" reworded to "2-year stability of the lesion" for clarity.
12) Amended and added items for data collection
13) Wording updated to reflect that the QUADAS-2 checklist was used for quality assessment, rather than the QUADAS checklist.
14) Rank Corrlation test performed to evaluate for the possibility of publication bias.
15) "Diagnostic yield" removed from "Approach to data synthesis" section
16) Approach to data synthesis updated per Cochrane manual recommendations
17) BI-RADS subgroup analysis added to the "Analysis of subgroups or subsets" section.
18) "Type and method of review" updated to include "Systematic review" for clarity.
19) Anticipated completion date updated

References

1. Pillai, A., et al., *Diagnostic Accuracy of Shear-Wave Elastography for Breast Lesion Characterization in Women: A Systematic Review and Meta-Analysis*. J Am Coll Radiol, 2022. **19**(5): p. 625-634.e0.
2. Wiechmann, L. and L.C. Friedlander, *Management of Radiographic Lesions of the Breast*. Surgical Clinics of North America, 2022. **102**(6): p. 1031-1041.
3. Skloot, R., *Taboo Organ: How a Pitt Alum Refused to Let Mammography Be Ignored*. Pitt Med Health, 2001.
4. *Practice Bulletin Number 179: Breast Cancer Risk Assessment and Screening in Average-Risk Women*. Obstet Gynecol, 2017. **130**(1): p. e1-e16.
5. Sickles EA, D.O.C., Bassett LW, et al. , *ACR BI-RADS® Mammography*. , in *ACR BI-RADS® Atlas, Breast Imaging Reporting and Data System*. . 2013, American College of Radiology: Reston, VA.
6. Mendelson, E.B., W.A. Berg, and C.R. Merritt, *Toward a standardized breast ultrasound lexicon, BI-RADS: ultrasound*. Semin Roentgenol, 2001. **36**(3): p. 217-25.
7. Corsetti, V., et al., *Role of ultrasonography in detecting mammographically occult breast carcinoma in women with dense breasts*. Radiol Med, 2006. **111**(3): p. 440-8.
8. Houssami, N., et al., *Sydney Breast Imaging Accuracy Study: Comparative sensitivity and specificity of mammography and sonography in young women with symptoms*. AJR Am J Roentgenol, 2003. **180**(4): p. 935-40.
9. Raskind, R., *Diagnostic ultrasonography*. J Am Geriatr Soc, 1965. **13**(10): p. 887-92.
10. Patey, S.J. and J.P. Corcoran, *Physics of ultrasound*. Anaesthesia & Intensive Care Medicine, 2021. **22**(1): p. 58-63.
11. Merritt, C.R.B., *Physics of Ultrasound*, in *Diagnostic ultrasound* D.L. Carol M. Rumack, Editor. 2018, Elsevier Philadelphia, PA. p. 1-33.
12. Nowicki, A. and K. Dobruch-Sobczak, *Introduction to ultrasound elastography*. J Ultrason, 2016. **16**(65): p. 113-24.
13. Morgan M, V.Z., Murphy A, et al. , *Acoustic impedance*. Radiopaedia.org 2022.
14. O'Gorman P, C.I., Knipe H, , *Propagation speed*. Radiopaedia.org 2021.
15. Carroll D, B.D., Murphy A, *Grey scale imaging (ultrasound)*. Radiopaedia.org 2020.
16. Yi, A., et al., *Addition of Screening Breast US to Digital Mammography and Digital Breast Tomosynthesis for Breast Cancer Screening in Women at Average Risk*. Radiology, 2021. **298**(3): p. 568-575.
17. Woods, R.W., et al., *The mammographic density of a mass is a significant predictor of breast cancer*. Radiology, 2011. **258**(2): p. 417-25.
18. Jordan, V., M. Khan, and D. Prill, *Breast Cancer Screening: Why Can't Everyone Agree?* Primary Care: Clinics in Office Practice, 2019. **46**(1): p. 97-115.
19. Huang, N., et al., *The Efficacy of Clinical Breast Exams and Breast Self-Exams in Detecting Malignancy or Positive Ultrasound Findings*. Cureus, 2022. **14**(2): p. e22464.

20. Gennisson, J.L., et al., *Ultrasound elastography: Principles and techniques*. Diagnostic and Interventional Imaging, 2013. **94**(5): p. 487-495.
21. Samani, A., J. Zubovits, and D. Plewes, *Elastic moduli of normal and pathological human breast tissues: an inversion-technique-based investigation of 169 samples*. Phys Med Biol, 2007. **52**(6): p. 1565-76.
22. Goddi, A., M. Bonardi, and S. Alessi, *Breast elastography: A literature review*. J Ultrasound, 2012. **15**(3): p. 192-8.
23. Dietrich, C.F., et al., *Strain Elastography - How To Do It?* Ultrasound Int Open, 2017. **3**(4): p. E137-e149.
24. Jeong, W.K., et al., *Principles and clinical application of ultrasound elastography for diffuse liver disease*. Ultrasonography, 2014. **33**(3): p. 149-60.
25. Glozman, T. and H. Azhari, *A Method for Characterization of Tissue Elastic Properties Combining Ultrasonic Computed Tomography With Elastography*. Journal of Ultrasound in Medicine, 2010. **29**(3): p. 387-398.
26. Cacko, D. and M. Lewandowski, *Shear Wave Elastography Implementation on a Portable Research Ultrasound System: Initial Results*. Applied Sciences, 2022. **12**(12): p. 6210.
27. Castera, L., X. Forns, and A. Alberti, *Non-invasive evaluation of liver fibrosis using transient elastography*. J Hepatol, 2008. **48**(5): p. 835-47.
28. Sandrin, L., et al., *Transient elastography: a new noninvasive method for assessment of hepatic fibrosis*. Ultrasound Med Biol, 2003. **29**(12): p. 1705-13.
29. Lee, S.M., et al., *Liver fibrosis staging with a new 2D-shear wave elastography using comb-push technique: Applicability, reproducibility, and diagnostic performance*. PLoS One, 2017. **12**(5): p. e0177264.
30. Song, P., et al., *Comb-push ultrasound shear elastography (CUSE): a novel method for two-dimensional shear elasticity imaging of soft tissues*. IEEE Trans Med Imaging, 2012. **31**(9): p. 1821-32.
31. Sigrist, R.M.S., et al., *Ultrasound Elastography: Review of Techniques and Clinical Applications*. Theranostics, 2017. **7**(5): p. 1303-1329.
32. Brief, S.N., *Shear wave elastography with VTIQ: A new tool to diagnose parathyroid adenomas*. Applied Radiology, 2016.
33. Zengel, P., F. Notter, and D.A. Clevert, *VTIQ and VTQ in combination with B-mode and color Doppler ultrasound improve classification of salivary gland tumors, especially for inexperienced physicians*. Clin Hemorheol Microcirc, 2018. **70**(4): p. 457-466.
34. Shin, K., et al., *Tomosynthesis-Guided Core Biopsy of the Breast: Why and How to Use it*. J Clin Imaging Sci, 2018. **8**: p. 28.
35. Nguyen, D.L., et al., *Disparities Associated With Patient Adherence to BI-RADS 3 Assessment Follow-up Recommendations for Mammography and Ultrasound*. J Am Coll Radiol, 2022. **19**(12): p. 1302-1309.
36. Vandromme, M.J., H. Umphrey, and H. Krontiras, *Image-guided methods for biopsy of suspicious breast lesions*. Journal of Surgical Oncology, 2011. **103**(4): p. 299-305.
37. Chakrabarthi, S., *Stereotactic breast biopsy: A review & applicability in the Indian context*. Indian J Med Res, 2021. **154**(2): p. 237-247.

38. Berg, W.A., et al., *Shear-wave elastography improves the specificity of breast US: the BE1 multinational study of 939 masses*. Radiology, 2012. **262**(2): p. 435-49.
39. Bercoff, J., M. Tanter, and M. Fink, *Supersonic shear imaging: a new technique for soft tissue elasticity mapping*. IEEE Trans Ultrason Ferroelectr Freq Control, 2004. **51**(4): p. 396-409.
40. Tanter, M., et al., *Quantitative assessment of breast lesion viscoelasticity: initial clinical results using supersonic shear imaging*. Ultrasound in medicine & biology, 2008. **34 9**: p. 1373-86.
41. Rutter, C.M. and C.A. Gatsonis, *A hierarchical regression approach to meta-analysis of diagnostic test accuracy evaluations*. Statistics in Medicine, 2001. **20**(19): p. 2865-2884.
42. Harbord, R.M., et al., *A unification of models for meta-analysis of diagnostic accuracy studies*. Biostatistics, 2007. **8**(2): p. 239-51.
43. Chen, Y.P., et al., *Comparison of Virtual Touch Tissue Quantification and Virtual Touch Tissue Imaging Quantification for diagnosis of solid breast tumors of different sizes*. Clin Hemorheol Microcirc, 2016. **64**(2): p. 235-244.
44. Hong, S., et al., *Reproducibility and diagnostic performance of shear wave elastography in evaluating breast solid mass*. Clin Imaging, 2017. **44**: p. 42-45.
45. Yang, P., et al., *Can continuous scans in orthogonal planes improve diagnostic performance of shear wave elastography for breast lesions?* Technol Health Care, 2015. **23 Suppl 2**: p. S293-300.
46. Golatta, M., et al., *Evaluation of virtual touch tissue imaging quantification, a new shear wave velocity imaging method, for breast lesion assessment by ultrasound*. Biomed Res Int, 2014. **2014**: p. 960262.
47. Ianculescu, V., et al., *Added value of Virtual Touch IQ shear wave elastography in the ultrasound assessment of breast lesions*. Eur J Radiol, 2014. **83**(5): p. 773-7.
48. Ren, W.W., et al., *Two-dimensional shear wave elastography of breast lesions: Comparison of two different systems*. Clin Hemorheol Microcirc, 2017. **66**(1): p. 37-46.
49. Li, G., et al., *Performance of Shear Wave Elastography for Differentiation of Benign and Malignant Solid Breast Masses*. PLoS ONE, 2013. **8**(10).
50. Chen, L., et al., *Diagnostic performances of shear-wave elastography for identification of malignant breast lesions: a meta-analysis*. Japanese Journal of Radiology, 2014. **32**(10): p. 592-599.
51. Xue, Y., et al., *Benign and malignant breast lesions identification through the values derived from shear wave elastography: Evidence for the meta-analysis*. Oncotarget, 2017. **8**(51): p. 89173-89181.
52. Blank, M.A.B. and J.F. Antaki, *Breast Lesion Elastography Region of Interest Selection and Quantitative Heterogeneity: A Systematic Review and Meta-Analysis*. Ultrasound in Medicine and Biology, 2017. **43**(2): p. 387-397.
53. Li, D.D., et al., *Acoustic radiation force impulse elastography for differentiation of malignant and benign breast lesions: A meta-analysis*. International Journal of Clinical and Experimental Medicine, 2015. **8**(4): p. 4753-4761.

54. Liu, B., et al., *Elastography by acoustic radiation force impulse technology for differentiation of benign and malignant breast lesions: a meta-analysis*. J Med Ultrason (2001), 2016. **43**(1): p. 47-55.
55. Luo, J., et al., *Benefit of shear-wave elastography in the differential diagnosis of breast lesion: a diagnostic meta-analysis*. Medical Ultrasonography, 2018. **20**(1): p. 43-49.
56. Barr, R.G., et al., *WFUMB Guidelines and Recommendations for Clinical Use of Ultrasound Elastography: Part 2: Breast*. Ultrasound in Medicine and Biology, 2015. **41**(5): p. 1148-1160.
57. Barr, R.G., et al., *Diagnostic Performance and Accuracy of the 3 Interpreting Methods of Breast Strain Elastography: A Systematic Review and Meta-analysis*. Journal of Ultrasound in Medicine, 2019. **38**(6): p. 1397-1404.
58. Tay, I.W.M., et al., *Shear wave versus strain elastography of breast lesions—The value of incorporating boundary tissue assessment*. Clinical Imaging, 2022. **82**: p. 228-233.
59. Cantisani, V., et al., *US-Elastography for Breast Lesion Characterization: Prospective Comparison of US BIRADS, Strain Elastography and Shear wave Elastography*. Ultraschall in der Medizin, 2021. **42**(5): p. 533-540.
60. Barr, R.G. and Z. Zhang, *Effects of precompression on elasticity imaging of the breast: Development of a clinically useful semiquantitative method of precompression assessment*. Journal of Ultrasound in Medicine, 2012. **31**(6): p. 895-902.
61. Barr, R.G. and Z. Zhang, *Shear-wave elastography of the breast: Value of a quality measure and comparison with strain elastography*. Radiology, 2015. **275**(1): p. 45-53.
62. Barr, R.G., *Breast Elastography: How to Perform and Integrate Into a "Best-Practice" Patient Treatment Algorithm*. Journal of Ultrasound in Medicine, 2020. **39**(1): p. 7-17.
63. Golatta, M., et al., *The potential of combined shear wave and strain elastography to reduce unnecessary biopsies in breast cancer diagnostics - An international, multicentre trial*. Eur J Cancer, 2022. **161**: p. 1-9.
64. Lin, X., et al., *Confirmed value of shear wave elastography for ultrasound characterization of breast masses using a conservative approach in chinese women: A large-size prospective multicenter trial*. Cancer Management and Research, 2018. **10**: p. 4447-4458.
65. Macaskill, P., *Chapter 10: Analysing and presenting results In: Deeks JJ, Bossuyt PM, Gatsonis C, eds. Cochrane Handbook for Systematic Reviews of Diagnostic Test Accuracy Version 1.0. The Cochrane Collaboration, 2010*.
66. Moon, J.H., et al., *Impact of region of interest (ROI) size on the diagnostic performance of shear wave elastography in differentiating solid breast lesions*. Acta Radiologica, 2018. **59**(6): p. 657-663.
67. Skerl, K., et al., *Influence of region of interest size and ultrasound lesion size on the performance of 2D shear wave elastography (SWE) in solid breast masses*. Clinical Radiology, 2015. **70**(12): p. 1421-1427.
68. Abdulmonaem, G., et al., *Supersonic shear waves quantitative elastography and kinetic magnetic resonance dynamic curve in discriminating BI-RADS 4 breast*

masses: A comparative study. The Egyptian Journal of Radiology and Nuclear Medicine, 2016. **47**.
69. Steinhauser, S., M. Schumacher, and G. Rücker, *Modelling multiple thresholds in meta-analysis of diagnostic test accuracy studies*. BMC medical research methodology, 2016. **16**(1): p. 1-15.
70. Yang, Y.P., et al., *Comparison of Virtual Touch Tissue Imaging & Quantification (VTIQ) and Virtual Touch Tissue Quantification (VTQ) for diagnosis of thyroid nodules*. Clin Hemorheol Microcirc, 2017. **65**(2): p. 137-149.
71. *What is an "AuntMinnie"?* . Available from: https://www.auntminnie.com/index.aspx?sec=abt.